Using Forward-Backward Drell-Yan Asymmetry in PDF determination

J. Fiaschi, E. Accomando, F. Hautmann, S. Moretti
& xFitter developers

Westfälische Wilhelms-Universität Münster

University of Southampton
School of Physics and Astronomy

Overview

- **State of art in modern PDFs determination**

- **Drell-Yan lepton pair production**

  - Cross section and Forward-Backward Asymmetry (AFB)
  - Properties of AFB
  - PDF and statistical uncertainty at the LHC Run-II and beyond

- **AFB in PDFs profiling**

  - Implementation of AFB in xFitter
  - Studies for PDFs profiling
  - Eigenvectors rotation

- **Conclusions**

Modern PDFs

- **State of art in modern PDFs determination**

- **Drell-Yan lepton pair production**

  - Cross section and Forward-Backward Asymmetry (AFB)
  - Properties of AFB
  - PDF and statistical uncertainty at the LHC Run-II and beyond

- **AFB in PDFs profiling**

  - Implementation of AFB in xFitter
  - Studies for PDFs profiling
  - Eigenvectors rotation

- **Conclusions**

Modern PDFs

- **Current status:**

  - LHC data from Run-I is an important input in PDF fits.
  - Drell-Yan Neutral Current data is included in the fits in the form of double differential distribution in the final state invariant mass and rapidity.
  - Charged Current (CC) data in the form of a lepton charge asymmetry is traditionally used for the determination of *d/u* quark PDF ratio, however due to the escaping neutrino, this observable can be used only "on-peak" $\left(\sqrt{\hat{s}} \simeq M_W\right)$
  - Correlations between *Z* and *W* cross sections are used to extract information of the strange quark content.
  - Recently Neutral Current triple differential distributions (invariant mass, rapidity and angle) have been released by ATLAS. ATLAS collaboration, JHEP 12, 059 (2017)
    PDF collaborations are indeed considering the effect of their inclusion in PDF fits.
    C. Willis, R. Brock, D. Hayden, T.J. Hou, J. Isaacson, C. Schmidt, C.P. Yuan, Phys. Rev. D 99, 054004 (2019)

- **Our proposal:**

  - Measurements of the Forward-Backward Asymmetry in the di-lepton final state will benefit future PDF fits.
  - We can exploit data in the invariant mass region around the *Z* peak as well as in the off-shell region.
  - The AFB features a remarkable reduction of systematic uncertainties.

Drell-Yan lepton pair production

- **State of art in modern PDFs determination**

- **Drell-Yan lepton pair production**

  - Cross section and Forward-Backward Asymmetry (AFB)
  - Properties of AFB
  - PDF and statistical uncertainty at the LHC Run-II and beyond

- **AFB in PDFs profiling**

  - Implementation of AFB in xFitter
  - Studies for PDFs profiling
  - Eigenvectors rotation

- **Conclusions**

Setup of Drell-Yan calculations

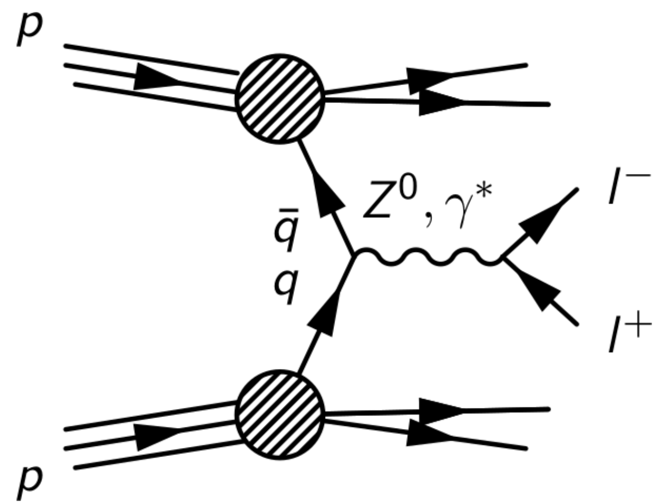

The focus is on the Drell-Yan Neutral Current (DY NC) process: $pp \to \ell^+\ell^-$

In particular we consider the di-electron final state because of its good experimental resolution (~ 1% of the invariant mass).

CMS collaboration, JHEP 04, 025 (2015)

The following results have been obtained with an independent code implementing a **LO** matrix element.

For the estimation of the expected number of events, and the related **statistical uncertainty**, we include **NNLO QCD** correction (residual scale uncertainty ~ few %) in the form of a mass dependent *K-factor.*

R. Hamberg, W.L. van Neerven and T. Matsuura, Nucl. Phys. B359, 343 (1991)

R. V. Harlander and W. B. Kilgore, Phys. Rev. Lett. 88, 201801 (2002)

Corrections from **NLO EW** are ~ 3.5% (not included here) ATLAS collaboration, JHEP 12, 059 (2017)

Experimental **acceptance** and **efficiency** of the electron channel are taken for the CMS detector.

CMS collaboration, JHEP 04, 025 (2015)

Following results available in:

E. Accomando, J. Fiaschi, F. Hautmann, S. Moretti, Phys. Rev. D 98, 013003 (2018), arXiv:1712.06318

E. Accomando, J. Fiaschi, F. Hautmann, S. Moretti, Eur. Phys. J C (2018) 78: 663, arXiv:1805.09239

Cross section measurements

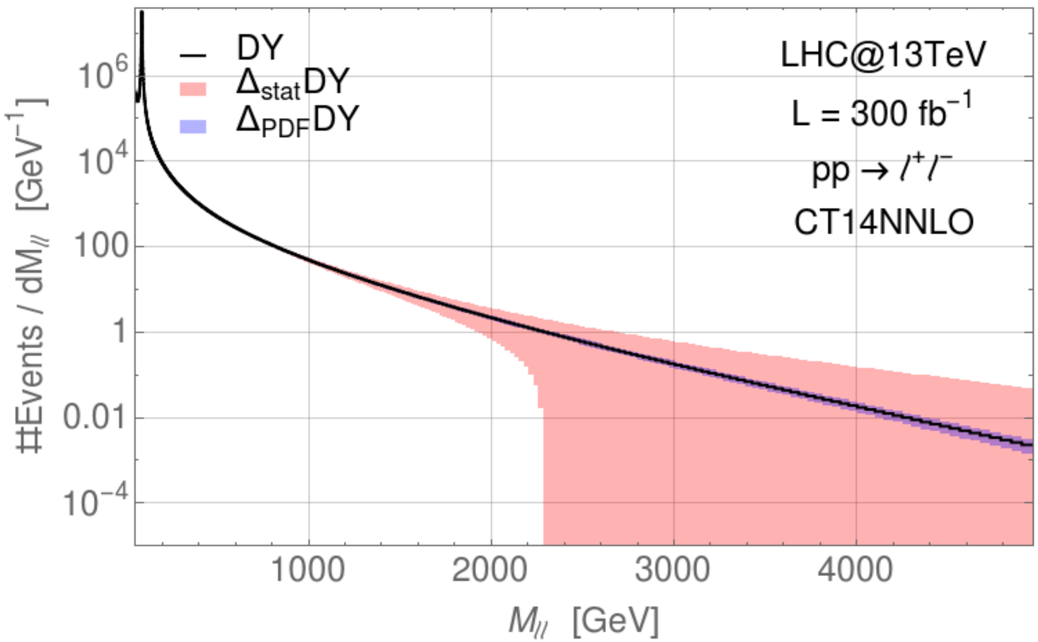

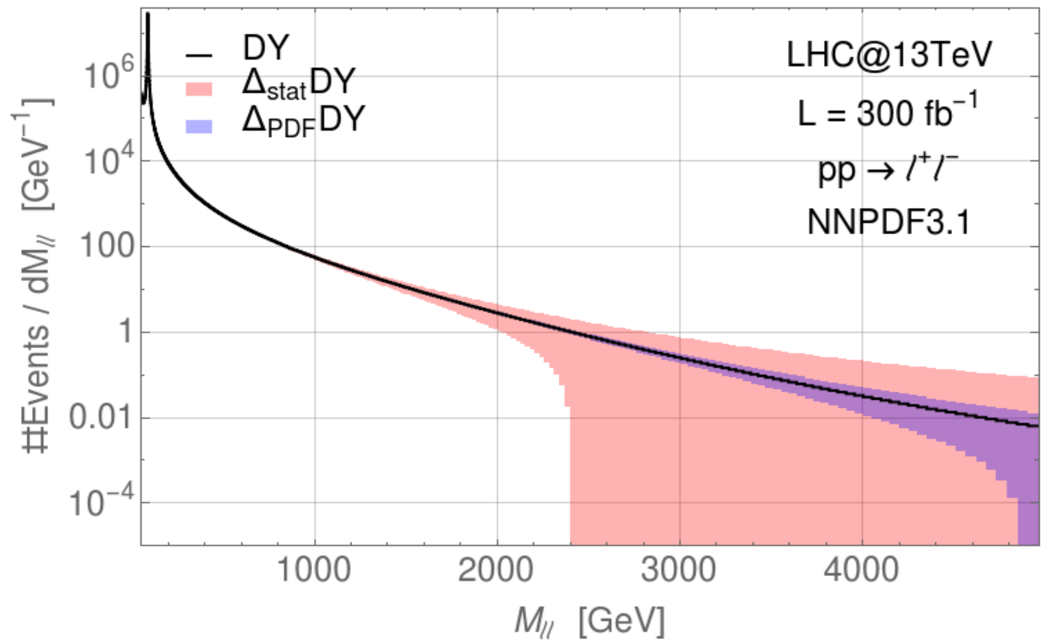

PDF uncertainties have been obtained following the prescription adopted within each PDF set (*replicas, eigenvectors, symmetric eigenvectors*).

The high invariant mass region is dominated by statistical uncertainties.

In the low invariant mass region around the *Z* peak, we can exploit the high statistics to perform very precise measurements.

Cross section measurements

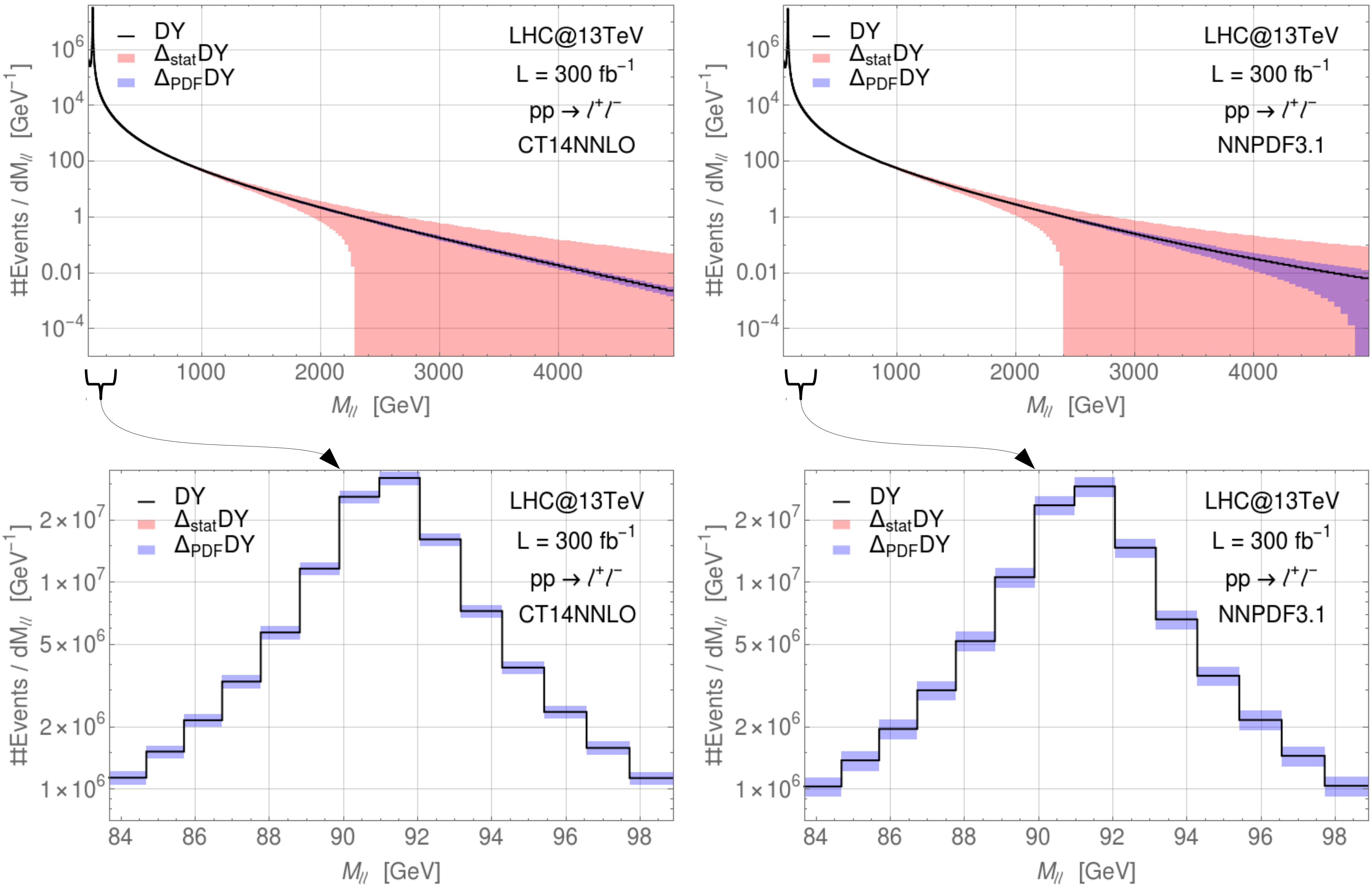

The Forward-Backward Asymmetry

$$\sigma_F = \int_0^1 \frac{d\sigma}{d\cos\theta} d\cos\theta \quad , \quad \sigma_B = \int_{-1}^0 \frac{d\sigma}{d\cos\theta} d\cos\theta$$

The angle $\boldsymbol{\theta}$ is defined in the partonic center of mass.

The direction of the incoming quark is defined by the boost of the di-lepton system

$$\boxed{A_{FB} = \frac{\sigma_F - \sigma_B}{\sigma_F + \sigma_B}}$$

At the LHC we can observe the reconstructed AFB*

It carries a complementary angular information (with respect to the cross section) and it is sensitive to different combination of the fermions chiral couplings:

$$\sum_{spin,pol} \left| \sum_i \mathcal{M}_i \right|^2 = \frac{\hat{s}^2}{3} \sum_{i,j} |P_i^* P_j| \left[\underbrace{\boxed{(1+\cos^2\theta) C_S^{i,j}}}_{\text{Cross section term}} + \underbrace{\boxed{2\cos\theta C_A^{i,j}}}_{\text{AFB term}} \right]$$

$$C_S^{i,j} = (a_{V_i} a_{V_j} + a_{A_i} a_{A_j})_L (a_{V_i} a_{V_j} + a_{A_i} a_{A_j})_Q$$

$$C_A^{i,j} = (a_{V_i} a_{A_j} + a_{A_i} a_{V_j})_L (a_{V_i} a_{A_j} + a_{A_i} a_{V_j})_Q$$

AFB* measurements

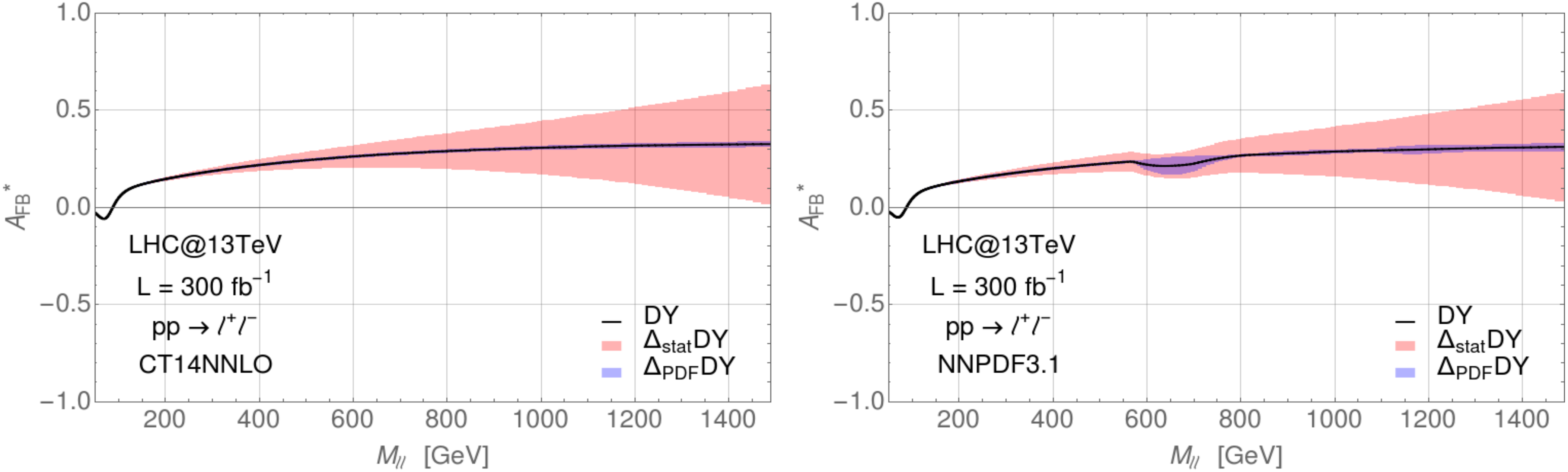

The ratio of cross sections in the definition of the **AFB** leads to a partial cancellation of systematic uncertainties.

Note: traditionally the **AFB** in hadron-hadron collision has been used for the determination of the weak mixing angle θ_w however the precision of measurements obtained at LEP exceeds by one order of magnitude the ones from the LHC. In this respect a combined analysis for the determination of both PDFs and θ_w would be recommended, or alternatively the independent and more precise value of θ_w obtained from LEP can be employed as input.

The high invariant mass region is affected by large statistical uncertainties.

Again we can exploit the invariant mass region around the *Z* peak to perform very precise measurements.

AFB* measurements

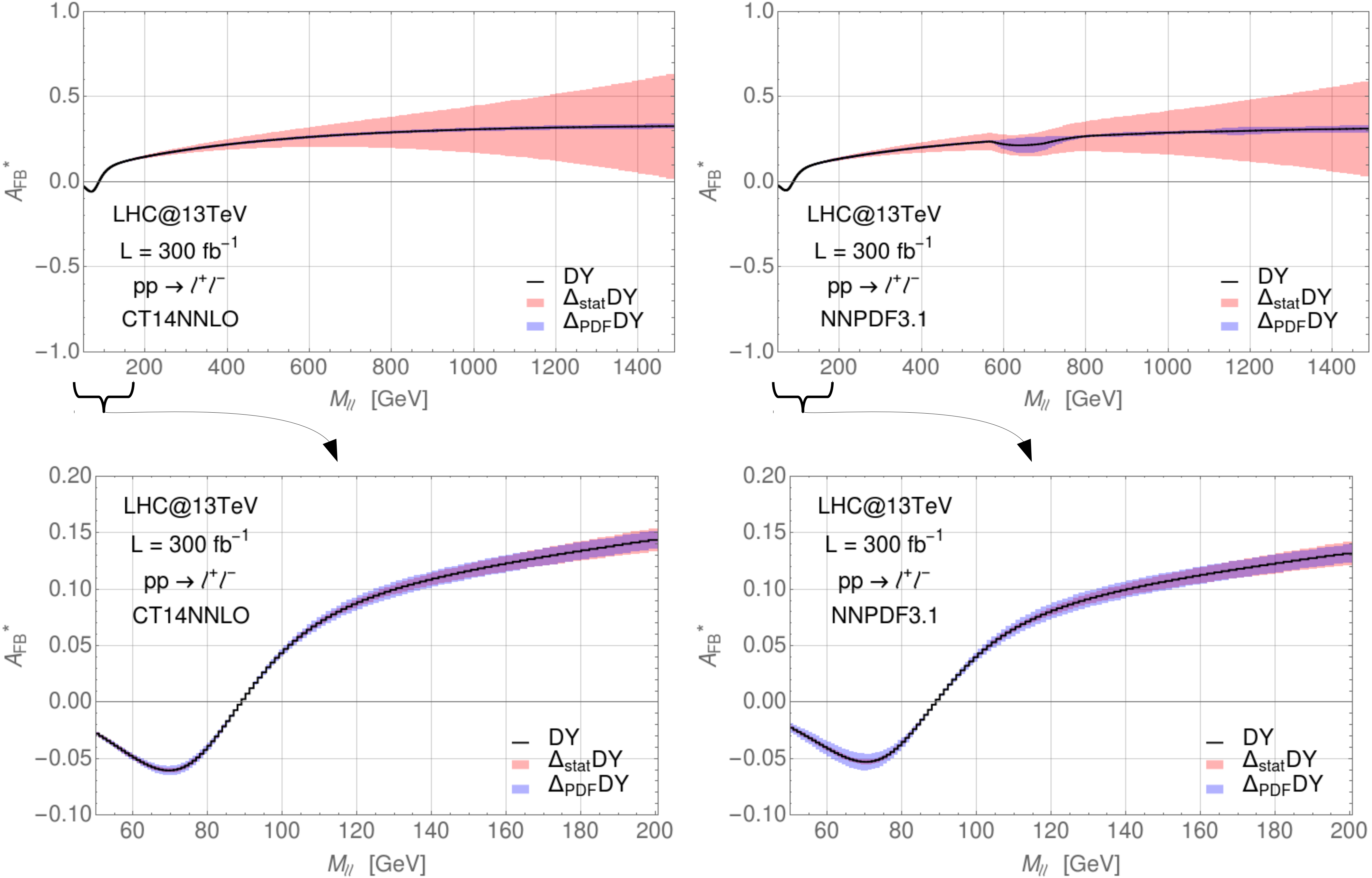

Run-I legacy

Double differential (invariant mass and rapidity) DY data from the LHC Run at 7 TeV and 8 TeV are an important input in the fit.

Comparing statistical and PDF error:

PDF error band includes the effect of factorization scale variation ($0.5M_{\ell\ell} \leq \mu_F \leq 2M_{\ell\ell}$)

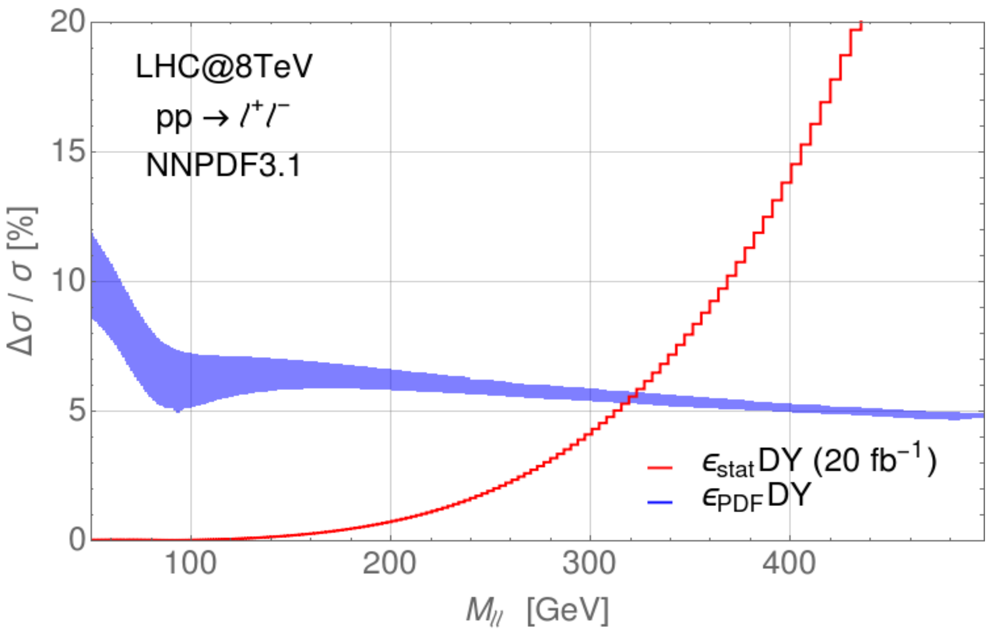

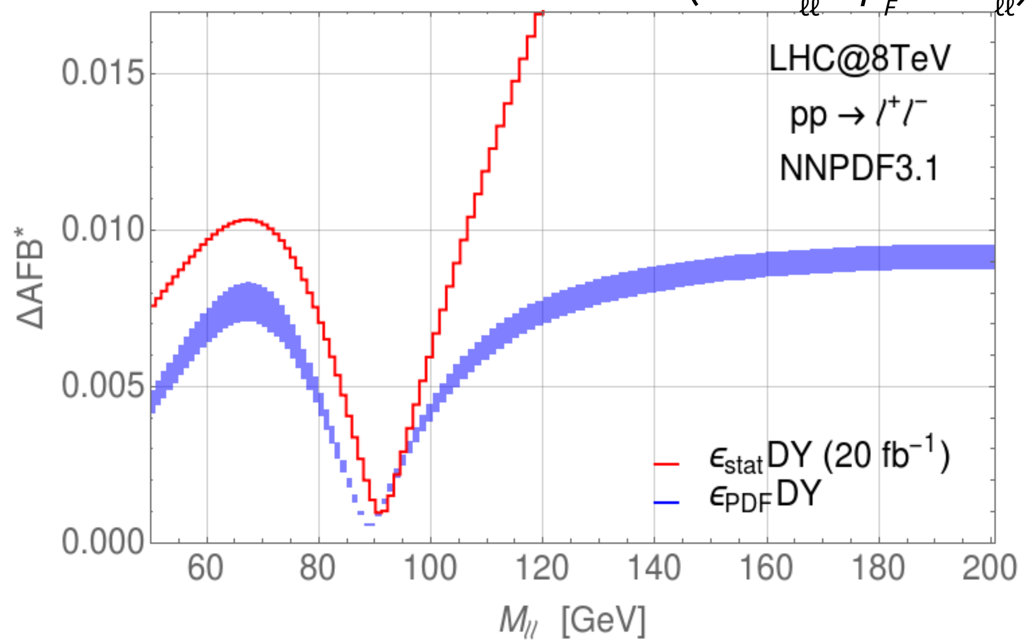

In the invariant mass region below ~ 320 GeV the inclusion of the LHC data could improve the fit.

The two sources of uncertainty are rather similar in magnitude, thus no gain in the PDF precision should be expected from the measurement of the AFB* at Run-I

LHC prospectives

Large amount of data will be recorded by the end of the Run-II and in the High Luminosity (HL) stages.

PDF fits can be improved exploiting <u>both differential cross section and AFB</u>*

PDF error band includes the effect of factorization scale variation
($0.5M_{\ell\ell} \leq \mu_F \leq 2M_{\ell\ell}$)

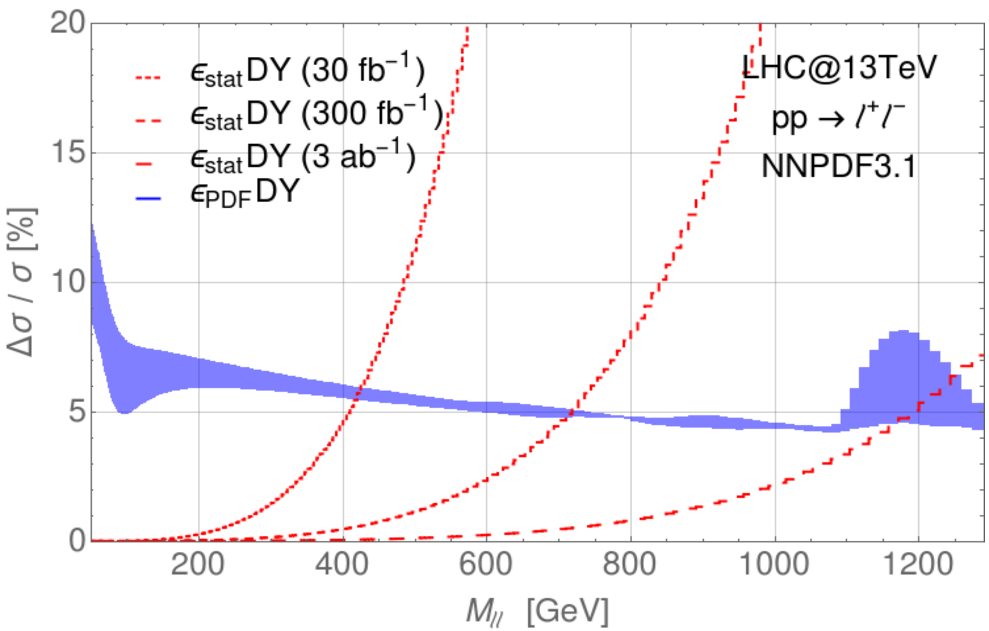

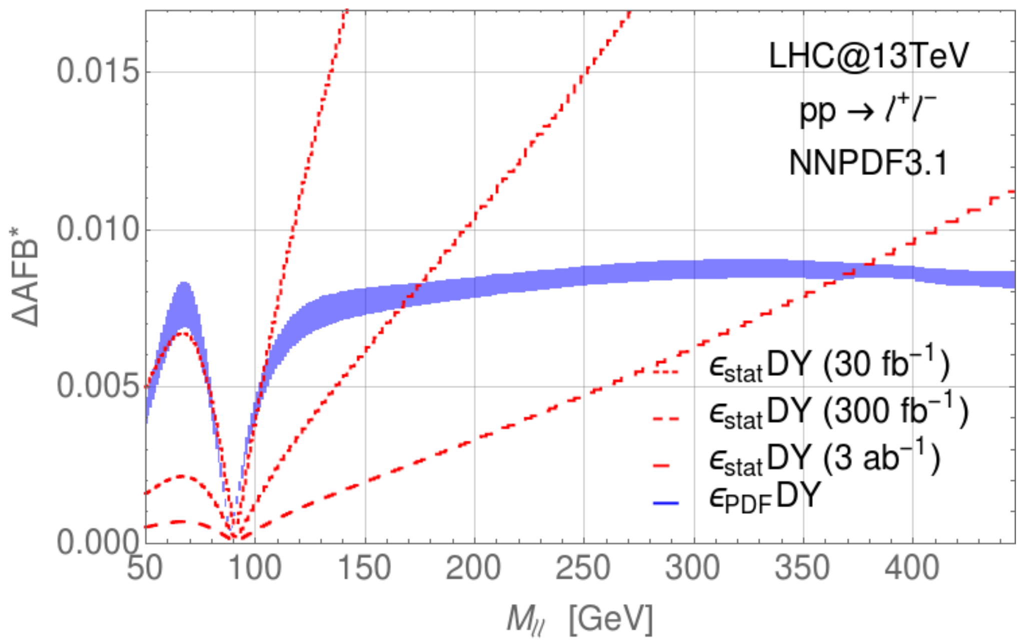

The region where the data can improve the PDF fit is further extended.

Also in the case of the AFB* distribution there is a region in which the statistical uncertainty is lower than the PDF error.

AFB in PDFs profiling

- **State of art in modern PDFs determination**

- **Drell-Yan lepton pair production**

  - Cross section and Forward-Backward Asymmetry (AFB)
  - Properties of AFB
  - PDF and statistical uncertainty at the LHC Run-II and beyond

- **AFB in PDFs profiling**

  - Implementation of AFB in xFitter
  - Studies for PDFs profiling
  - Eigenvectors rotation

- **Conclusions**

Setup of xFitter analysis

Datafiles with pseudo-data generated for many PDF sets with the following setup:

- AFB central values:
  120 bins of 1 GeV from 80 GeV to 200 GeV.
- Estimation of statistical uncertainty:
  at different integrated luminosities (*30 fb*$^{-1}$*, 300 fb*$^{-1}$ and *3000 fb*$^{-1}$)
  including detector acceptance and efficiency in the di-electron final state.
- Rapidity cuts:
  different lower rapidity cuts applied ($|Y| > 0$, $|Y| > 0.8$ and $|Y| > 1.5$)

Profiling exercise performed on 5 NNLO PDF sets:
ABMP16NNLO, CT14NNLO, HERA2.0NNLO, MMHT2014NNLO, NNPDF3.1NNLO (hessian set).

Results will be shown for 2 reference scales $\mathbf{Q^2 = 100\ GeV^2}$ and $\mathbf{Q^2 = M_Z^2\ GeV^2}$.

Reweighted eigenvectors are returned by xFitter and analysed with the **xFitter-draw** script.

PDF profiling

CT14 nnlo (L = 300 fb^{-1}) (Q^2 = 100 GeV^2)

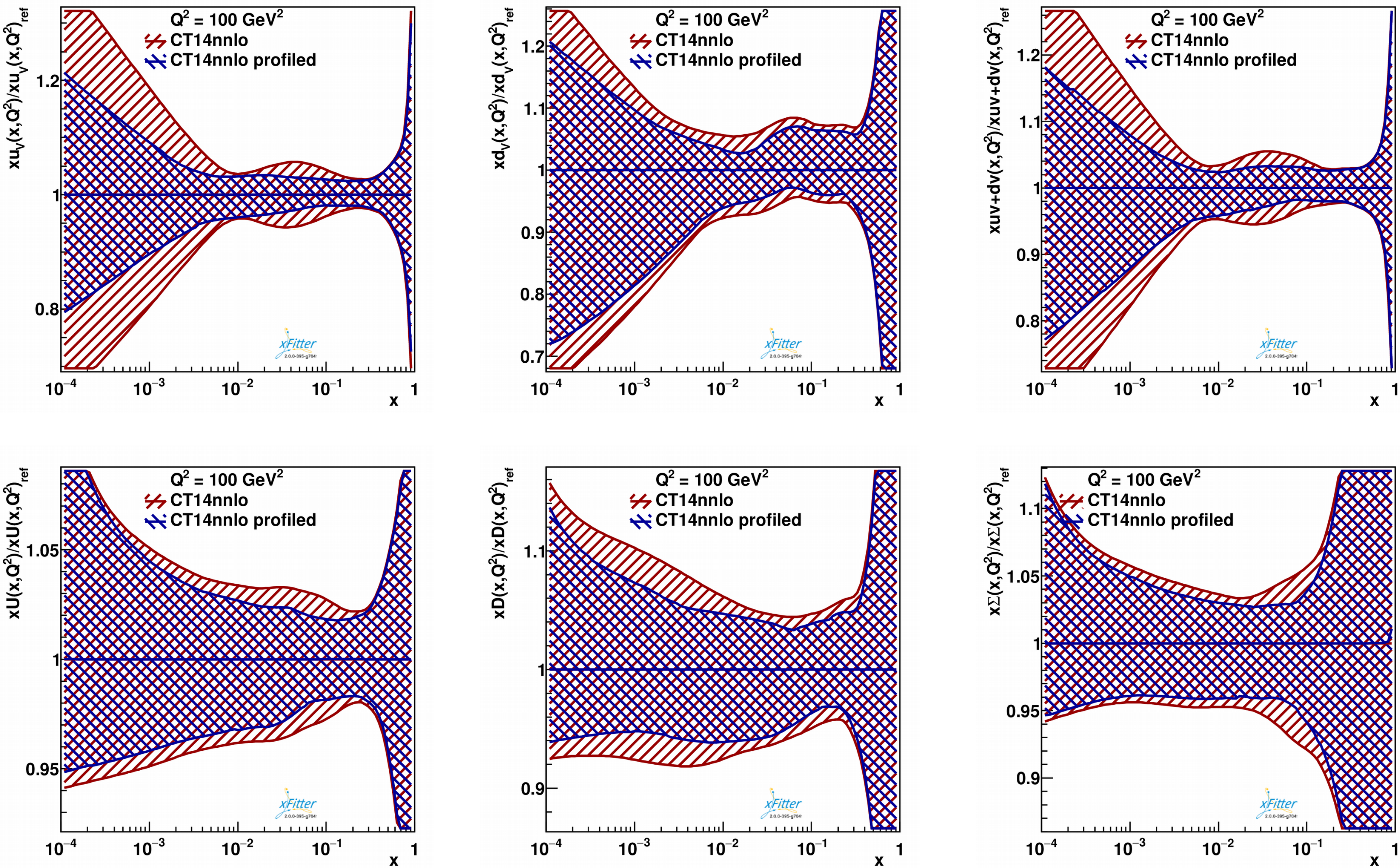

Juri Fiaschi *xFitter workshop* *18/03/2019*

PDF profiling

CT14 nnlo (L = 300 fb^{-1}) ($Q^2 = M_Z^2$ GeV^2)

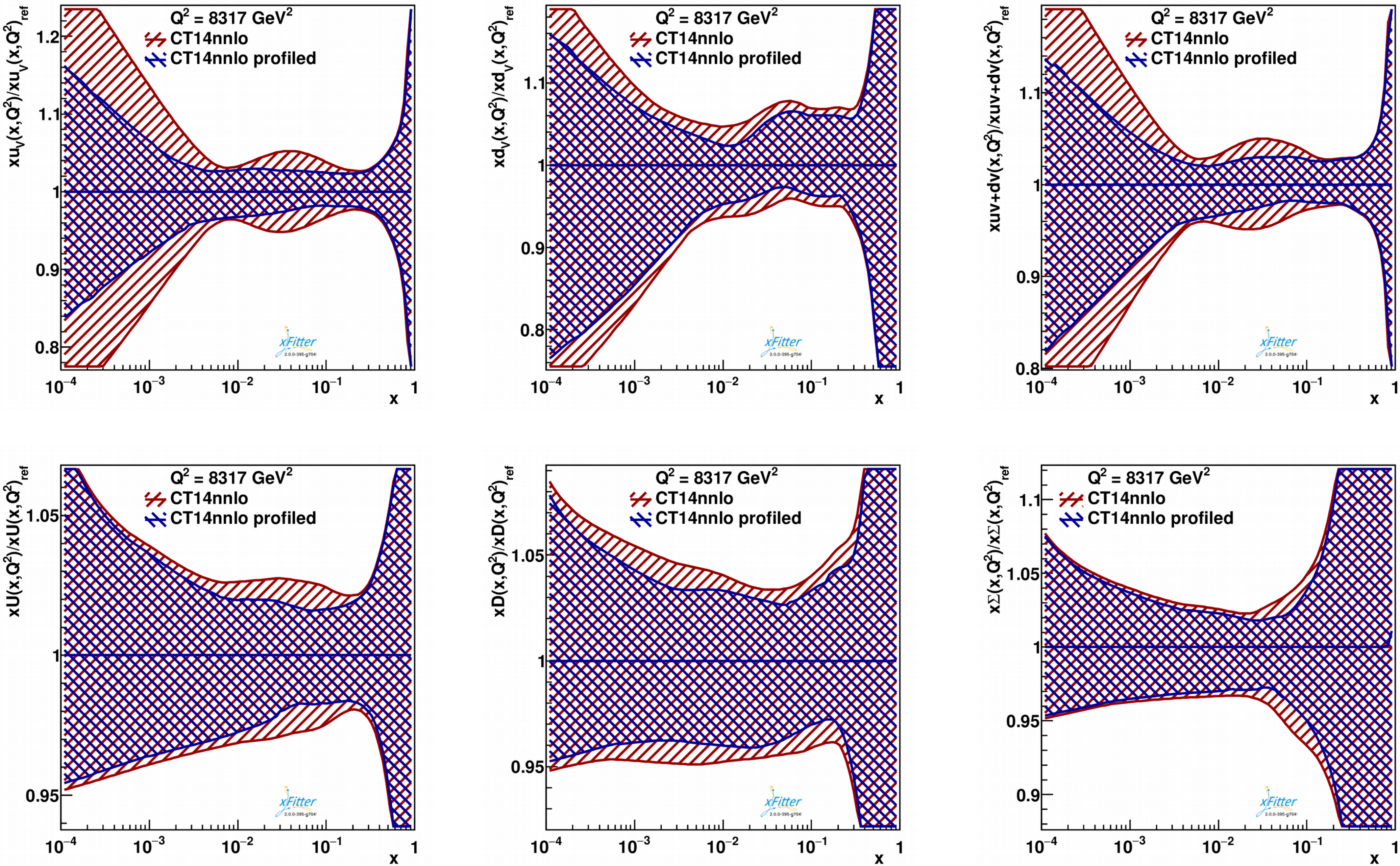

PDF profiling

<u>CT14 nnlo</u> (L = 30 fb^{-1}) **($Q^2 = M_Z^2$ GeV^2)**

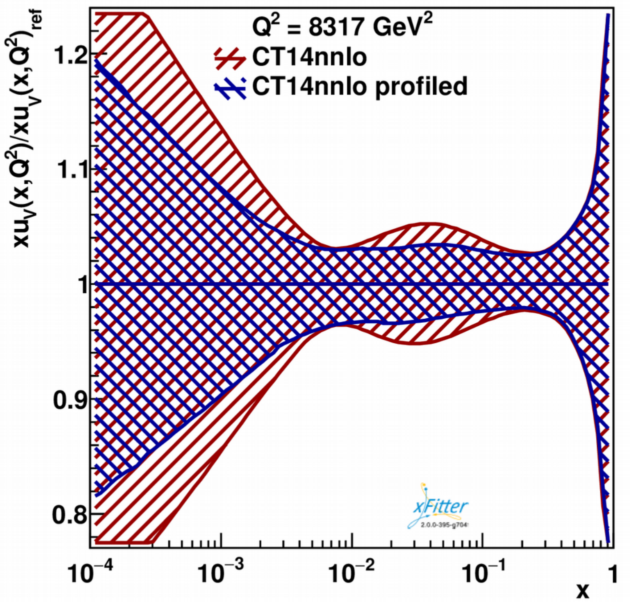

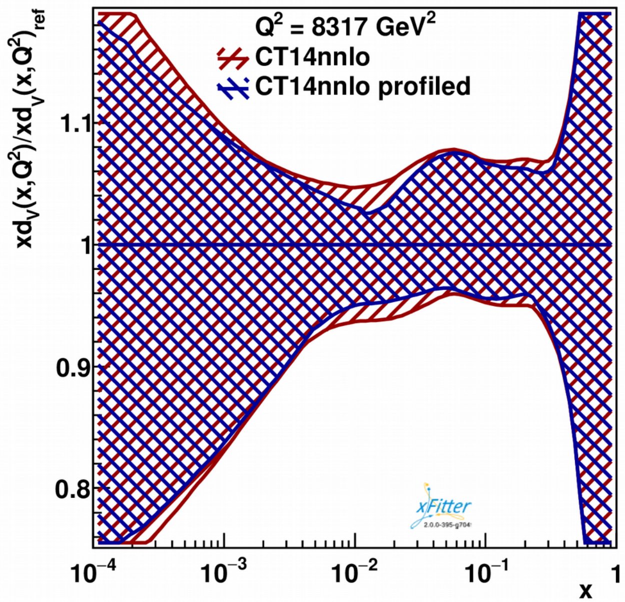

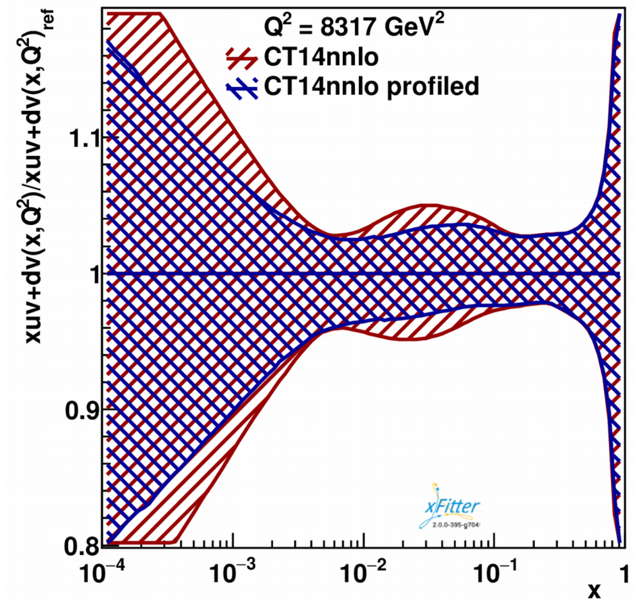

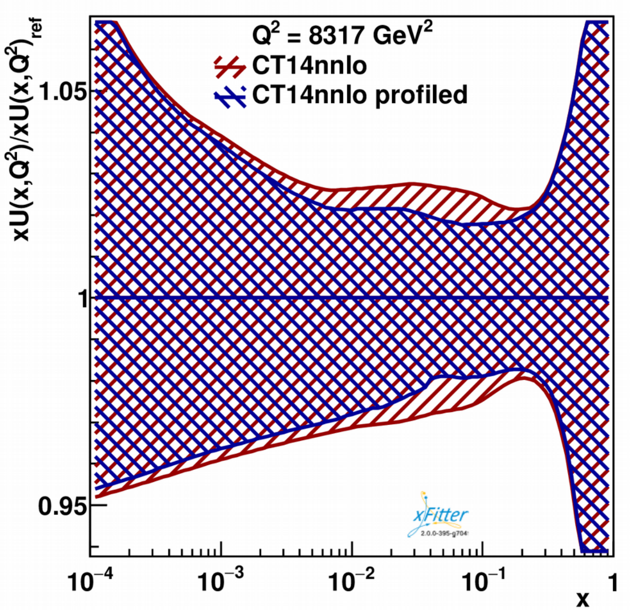

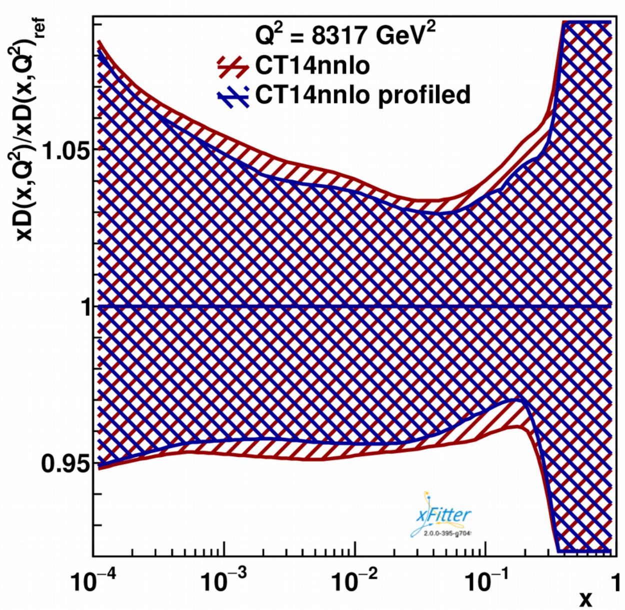

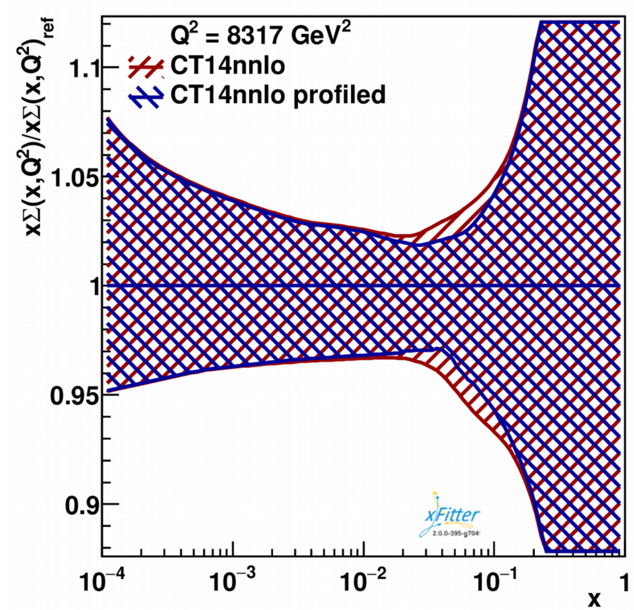

PDF profiling

CT14 nnlo (L = 3000 fb^{-1}) ($Q^2 = M_Z^2$ GeV^2)

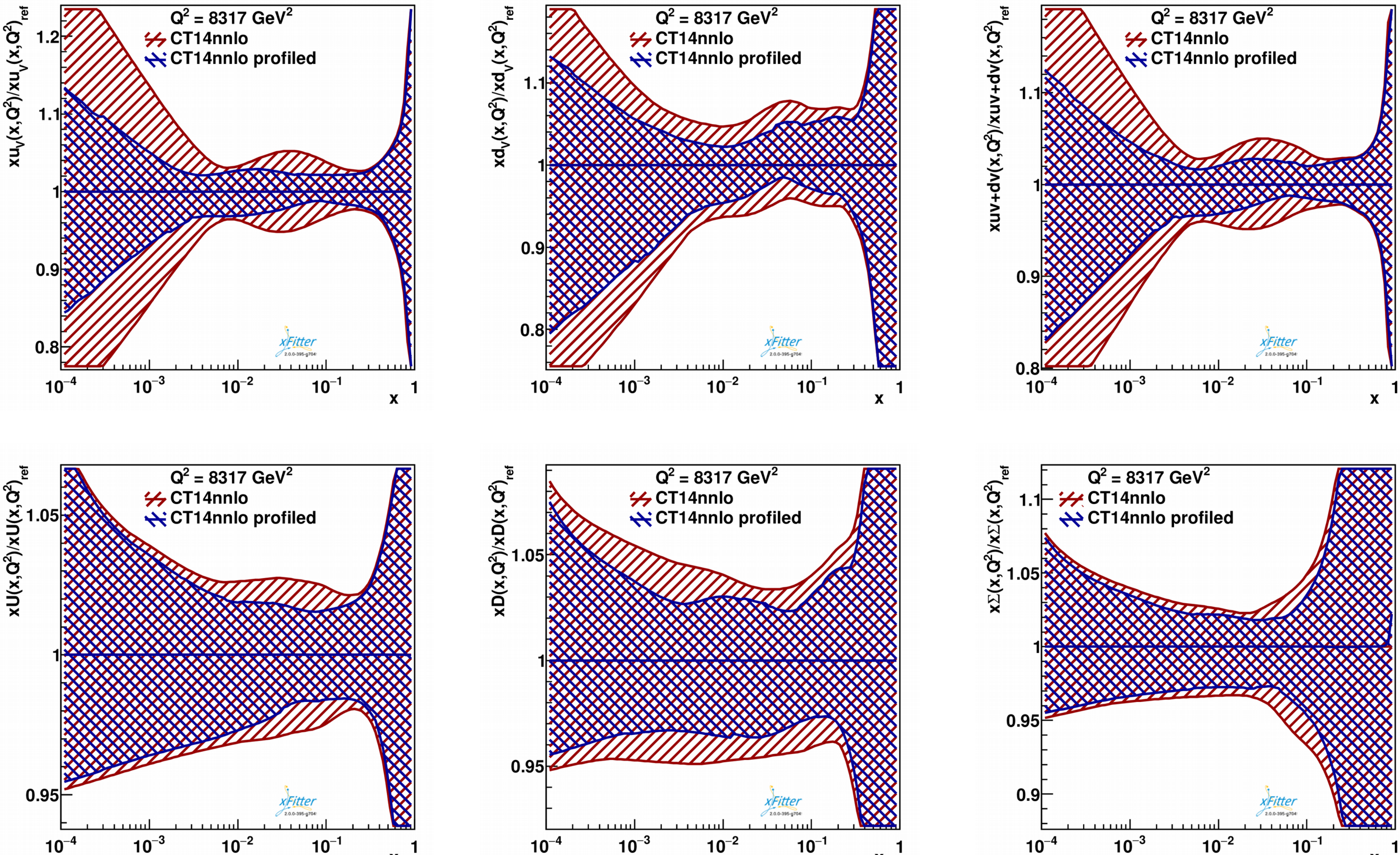

PDF profiling

NNPDF3.1 nnlo ($Q^2 = M_Z^2$ GeV^2) (L = 300 fb^{-1})

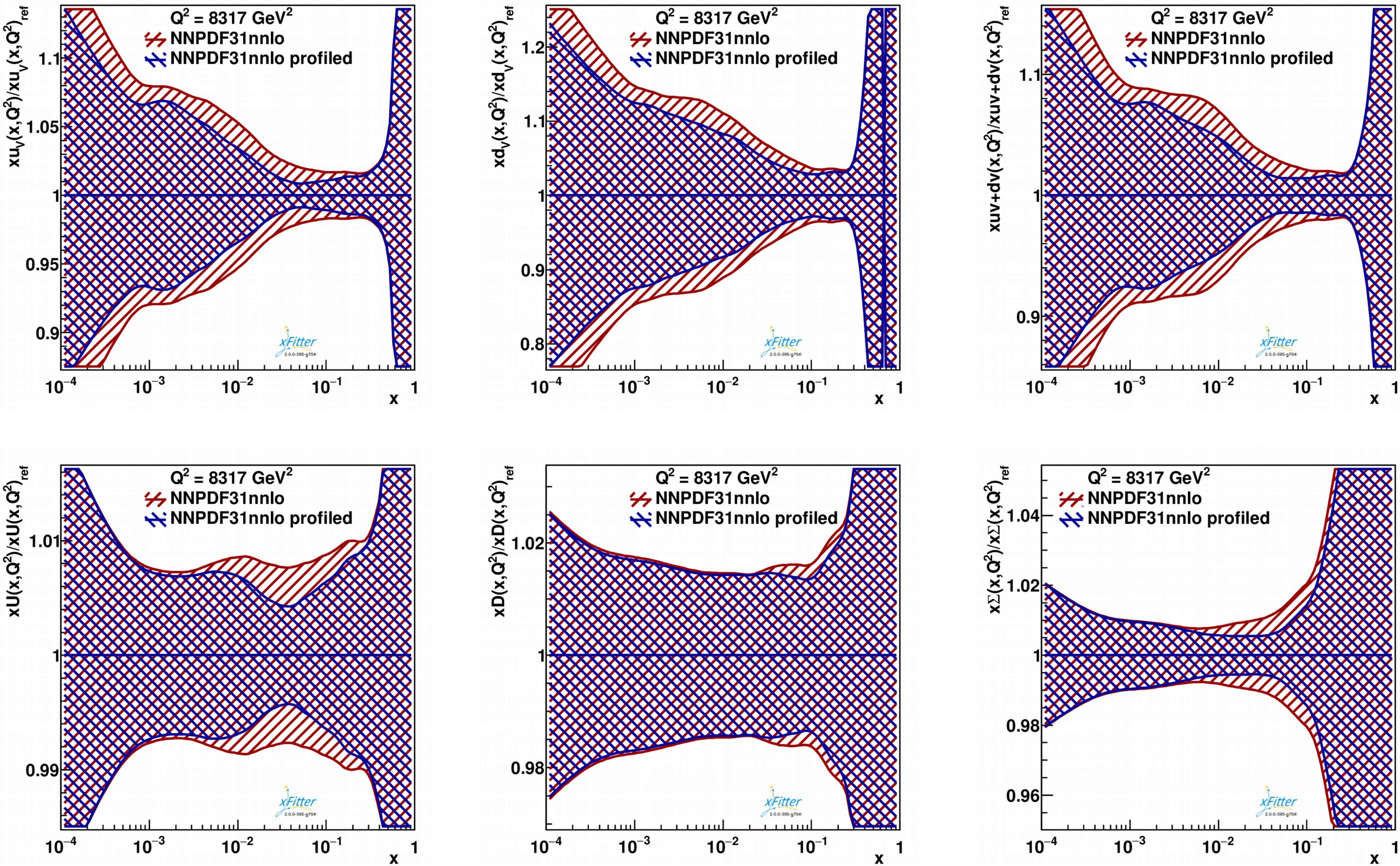

PDF profiling

MMHT2014 nnlo ($Q^2 = M_Z^2$ GeV^2) (L = 300 fb^{-1})

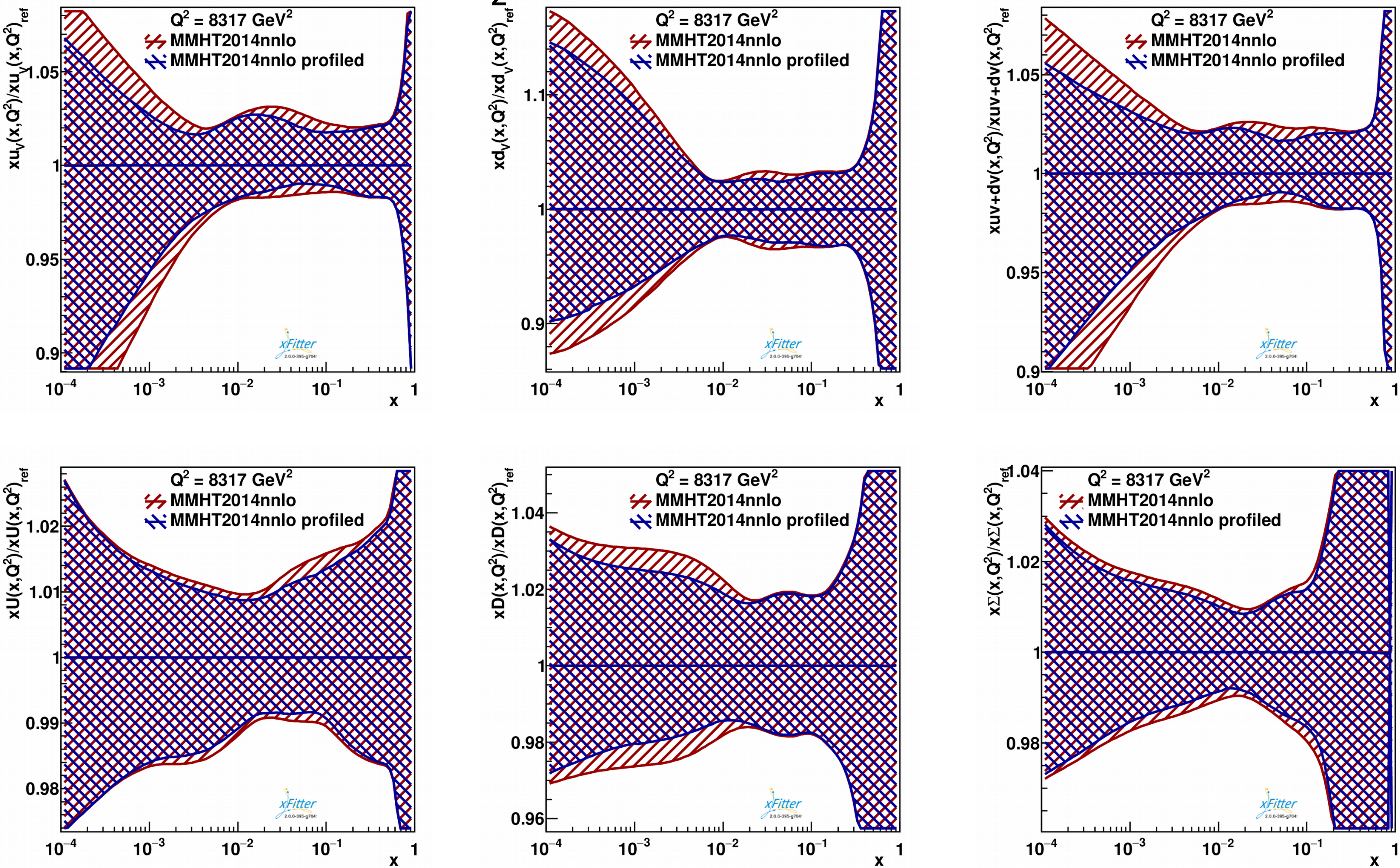

PDF profiling

<u>ABMP16 nnlo</u> ($Q^2 = M_Z^2$ GeV^2) (L = 300 fb^{-1})

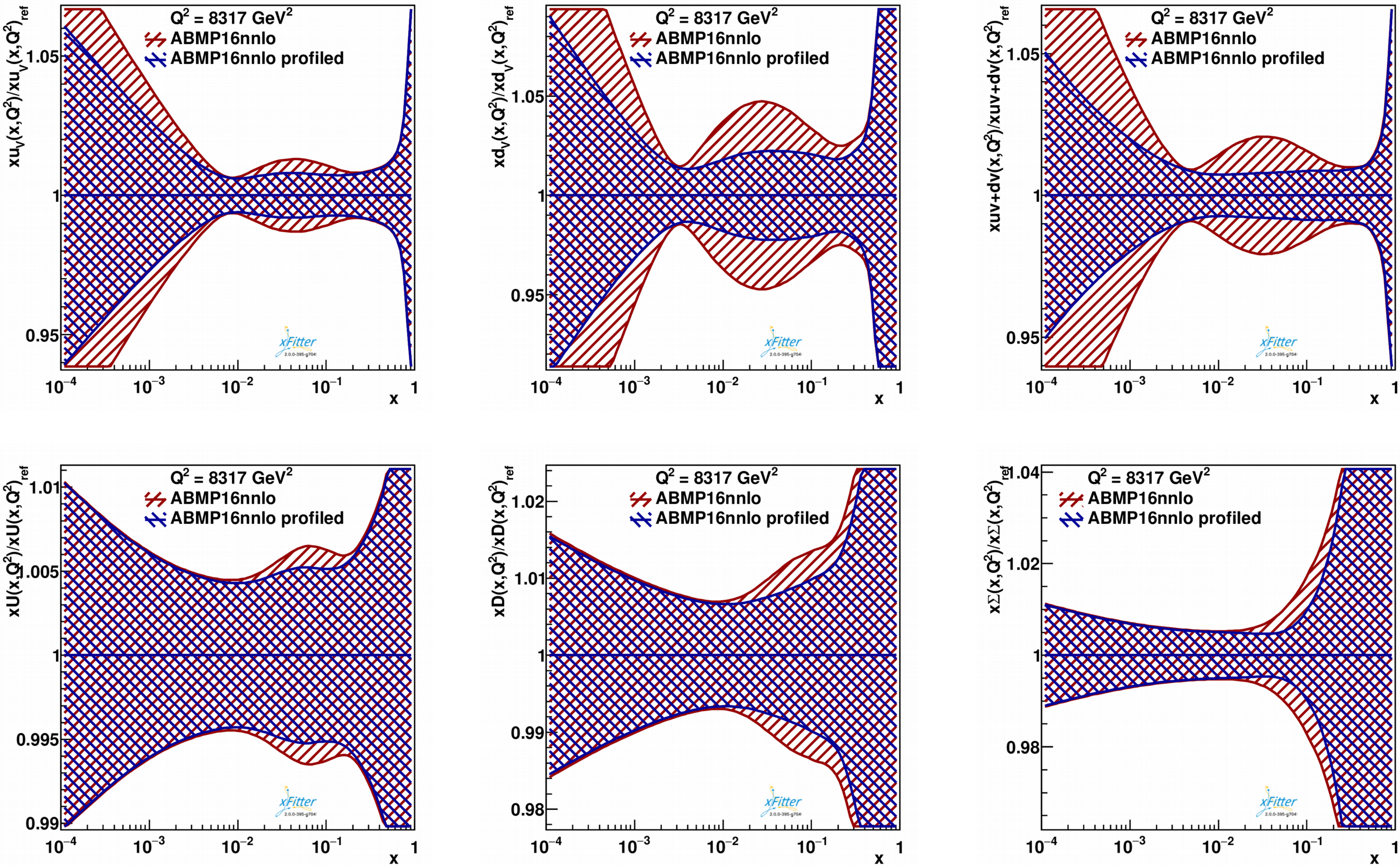

PDF profiling

HERA2.0 nnlo ($Q^2 = M_Z^2$ GeV^2) (L = 300 fb^{-1})

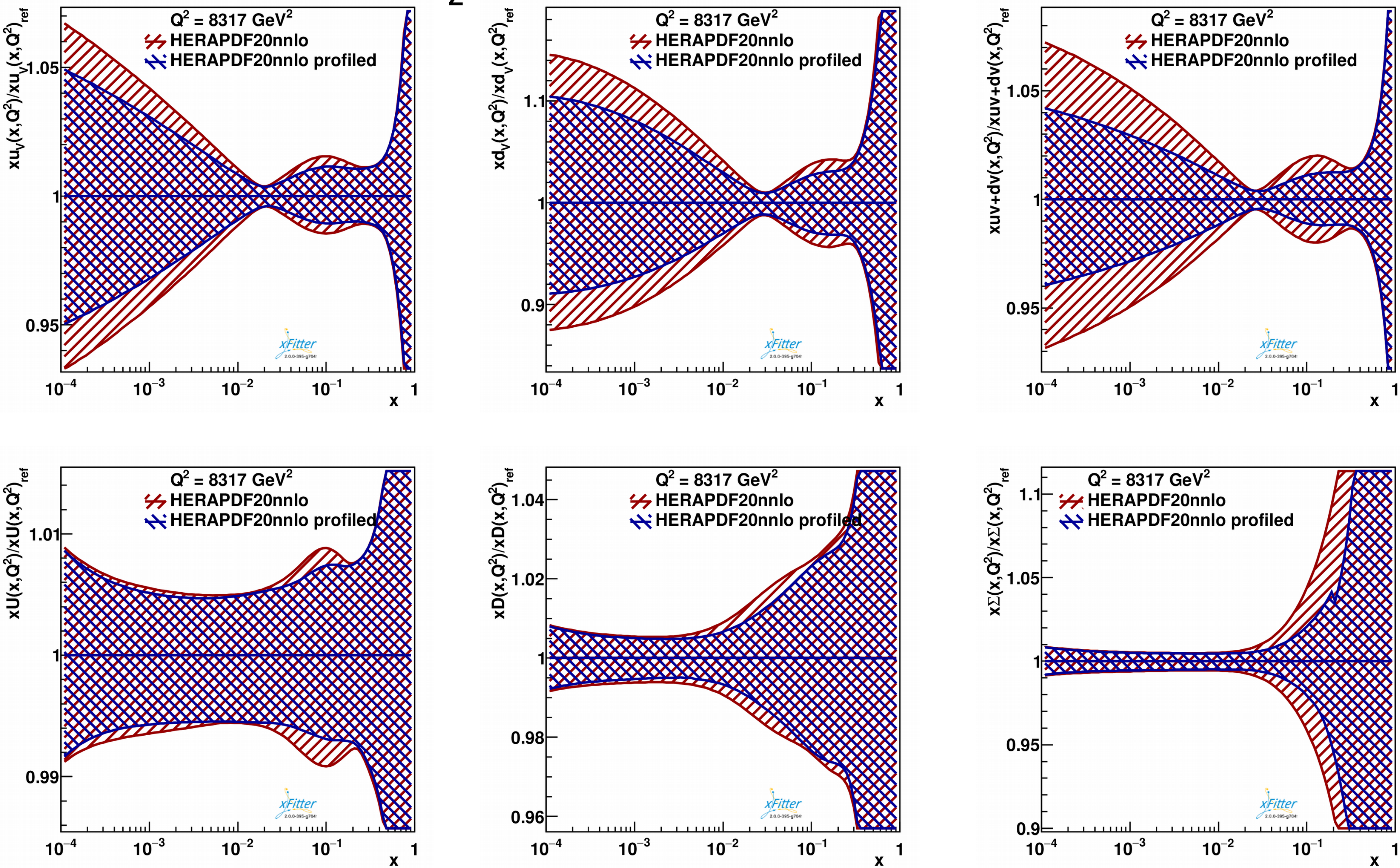

PDF profiling

HERA2.0 nnlo ($Q^2 = M_Z^2$ GeV^2) (L = 3000 fb^{-1}) |Y| > 0

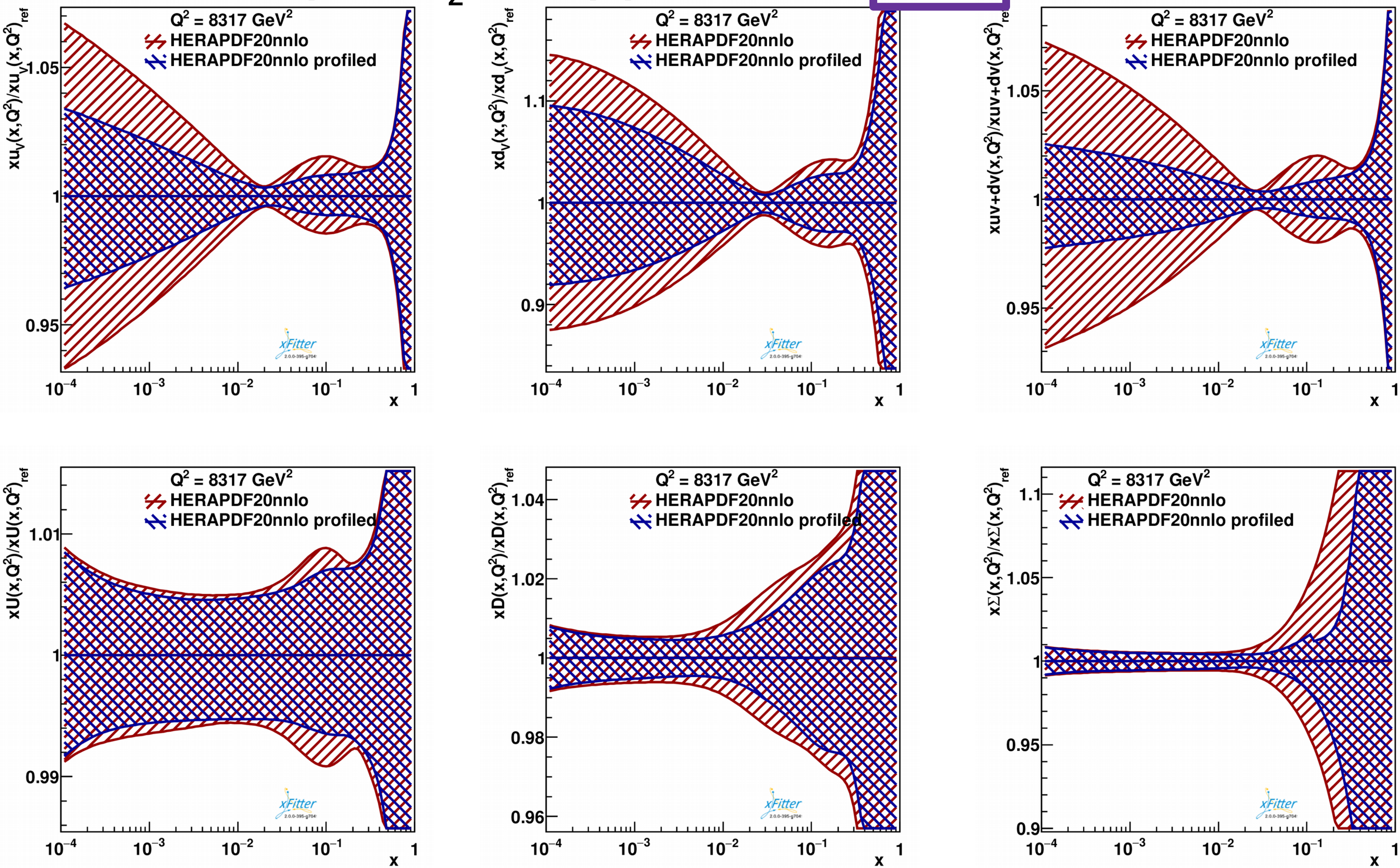

PDF profiling

HERA2.0 nnlo ($Q^2 = M_Z^2$ GeV^2) (L = 3000 fb^{-1}) |Y| > 0.8

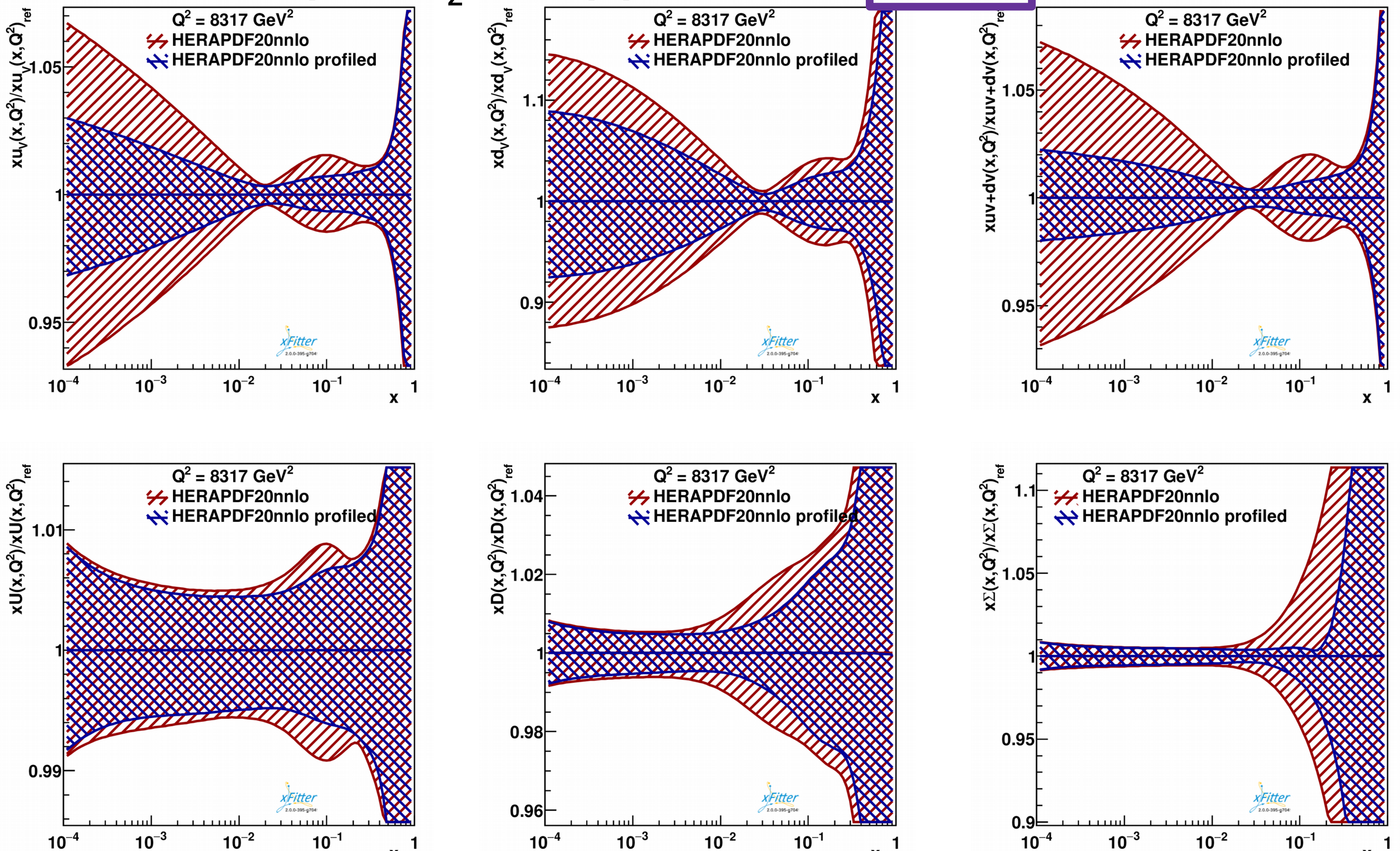

PDF profiling

<u>HERA2.0 nnlo</u> ($Q^2 = M_Z^2$ GeV^2) (L = 3000 fb^{-1}) |Y| > 1.5

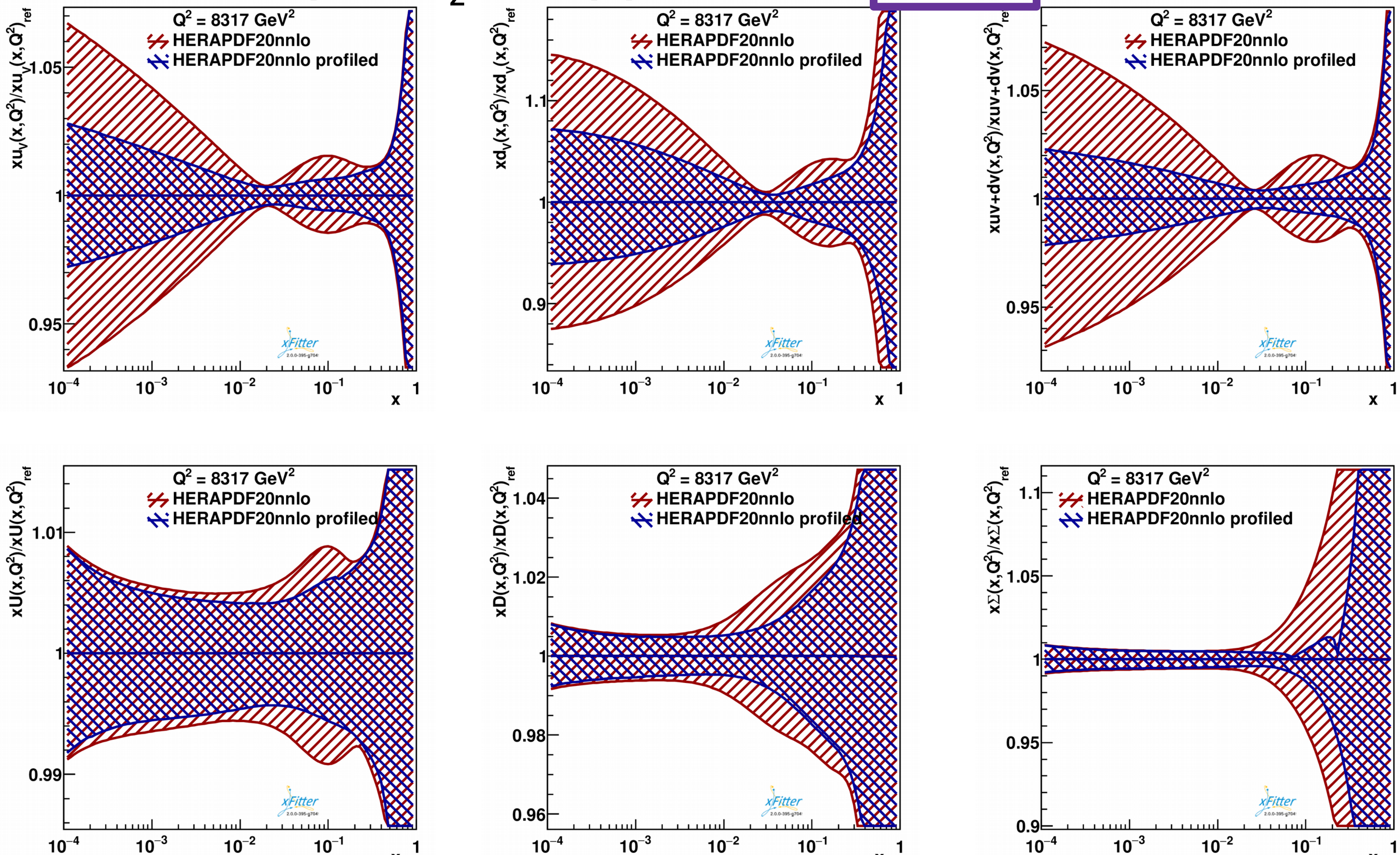

PDF profiling

Results of LO analysis:

Reduction of the uncertainties observed in *u*-valence and *d*-valence distributions.

Some PDF sets appear to benefit more from the inclusion of AFB data.

The PDF sets **ABMP16NNLO, CT14NNLO** and particularly **HERA2.0NNLO** experience a reduction of the uncertainties of few %.

MMHT2014NNLO and **NNPDF3.1NNLO** are less sensitive to the new data. The reduction of the uncertainties is of the order of 1 %.

AFB data in the high rapidity region has a noticeable effect on *u*- and *d*-quarks PDFs in the high-*x* region.

PDF eigenvectors rotation

The eigenvectors of a PDF set are rotated and sorted according to their sensitivity to the AFB data.

Procedure applied to the PDF sets most sensitive to the AFB data: **ABMP16NNLO, CT14NNLO** and **HERA2.0NNLO**.

The contribution of the first 4 and of the last eigenvectors to the PDF error bands of the physical partons' PDFs are plotted using the **xFitter-draw** script.

The pseudodata used in this analysis features no rapidity cut ($|Y| > 0$) and their statistical uncertainty corresponds to an integrated luminosity $L = 300\ fb^{-1}$.

PDF eigenvectors rotation

CT14nnlo ($Q^2 = M_Z^2$ GeV^2) **(Hessian eigenvectors)**

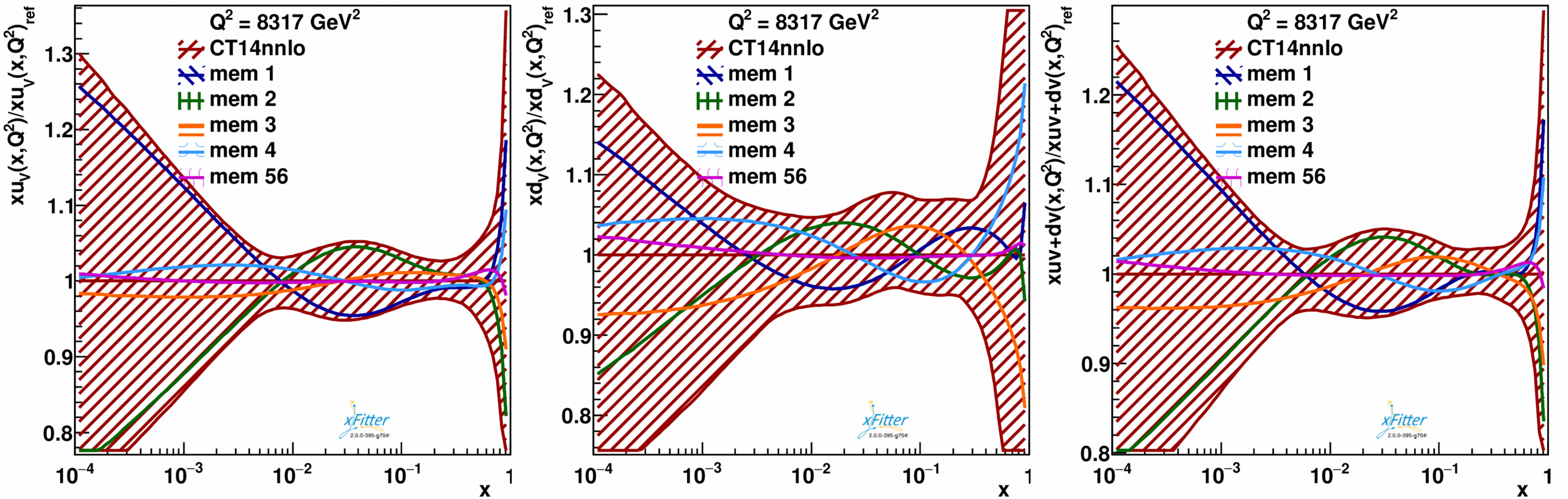

Dataset	CT14nnlo	mem 1	mem 2	mem 3	mem 4	mem 56
DY AFB	0 / 120	171 / 120	162 / 120	11 / 120	14 / 120	0.53 / 120
Correlated χ^2	0.000000038	0	0	0	0	0
Log penalty χ^2	-0.00	-7.11	+7.0	-0.43	+0.57	+0.45
Total χ^2 / dof	-0 / 120	164 / 106	169 / 106	10 / 106	14 / 106	0.98 / 106
χ^2 p-value	1.00	0.00	0.00	1.00	1.00	1.00

PDF eigenvectors rotation

<u>HERA2.0 nnlo</u> ($Q^2 = M_Z^2$ GeV^2) **(Hessian eigenvectors)**

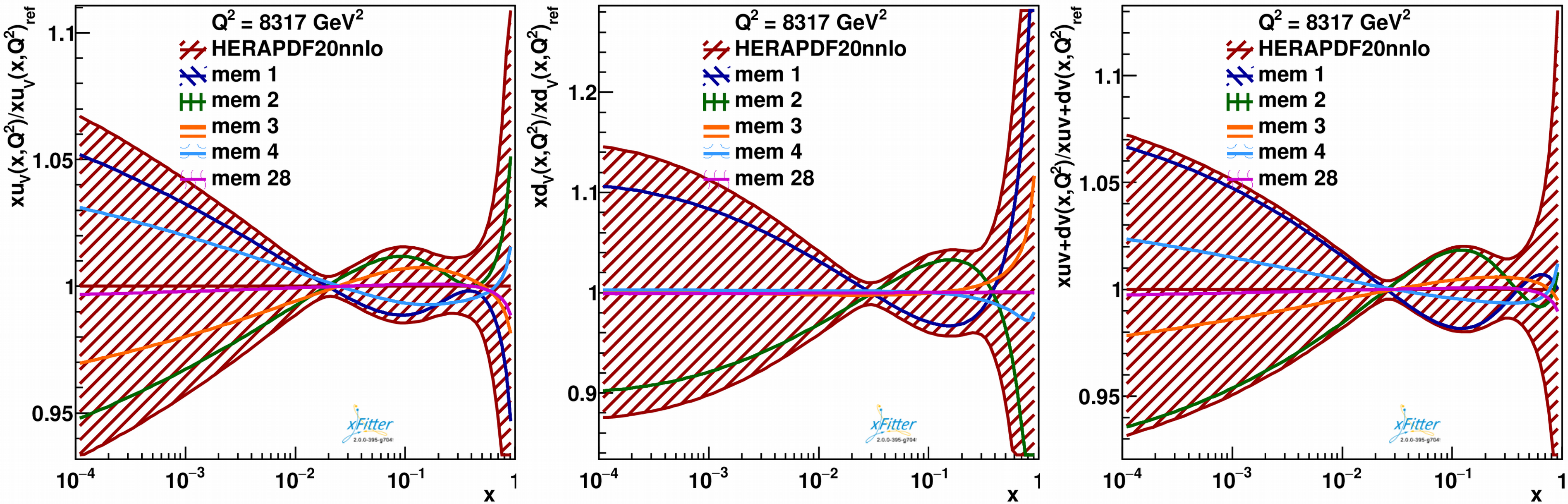

Dataset	HERAPDF20nnlo	mem 1	mem 2	mem 3	mem 4	mem 28
DY AFB	0 / 120	6.5 / 120	6.4 / 120	0.62 / 120	0.60 / 120	0 / 120
Correlated χ^2	0.000000038	0	0	0	0	0
Log penalty χ^2	+0.00	-1.65	+1.6	-0.15	+0.14	+0.01
Total χ^2 / dof	0 / 120	4.8 / 106	8.0 / 106	0.48 / 106	0.74 / 106	0.0100 / 106
χ^2 p-value	1.00	1.00	1.00	1.00	1.00	1.00

PDF eigenvectors rotation

Outcomes from eigenvectors rotation exercise:

- The dominant contribution to PDF error band comes from first eigenvectors.
- They mostly affect *u*- and *d*- valence quarks, but also *sea* quark PDFs (especially at high x ~ 0.1)
- Variation of *u*- and *d*- valence quarks PDFs are positively correlated.
- Variation of *sea* PDFs is negatively correlated to them (momentum sum rule).
- Best constrains on the PDF combination $u_v + d_v$

Conclusions

- **State of art in modern PDFs determination**

- **Drell-Yan lepton pair production**
  - Cross section and Forward-Backward Asymmetry (AFB)
  - Properties of AFB
  - PDF and statistical uncertainty at the LHC Run-II and beyond

- **AFB in PDFs profiling**
  - Implementation of AFB in xFitter
  - Studies for PDFs profiling
  - Eigenvectors rotation

- **Conclusions**

Conclusions

- Forthcoming data from LHC run-II and HL stages will achieve unprecedented statistical precision, and will be an important ingredient to further improve the determination of partons' PDFs, with particular mention to Drell-Yan data.
- Drell-Yan data in particular will provide important constrains. Traditionally this information is included in PDF fits in the form of differential cross section.
- We have shown that also the **Forward-Backward Asymmetry** observable in the invariant mass region around the Z peak will achieve a sufficient experimental precision to benefit future PDF fits.
- The AFB carries <u>extra information on the angular distribution</u> of events. Moreover it is a solid observable in terms of systematics which receive <u>large cancellations</u> in the ratio.
- AFB measurements can also be used to <u>discriminate between the different parametrisations</u> of the (anti)quark PDFs. In particular its discriminating potential increases when imposing lower rapidity cuts on the di-lepton system.

Conclusions

- We have implemented the AFB observable at LO into **xFitter**.
- We have analysed the potential of AFB pseudodata in the LHC run-II and HL setup in the profiling of selected PDF sets.
- We have considered different luminosities and applied rapidity cuts in order to study their effects in the reduction of PDF uncertainty bands.
- The result is a visible reduction of the uncertainties, especially for the valence up and down quarks. Smaller effects are visible in the sea quark distributions.
- This conclusion is also confirmed from the analysis of equivalent PDF sets whose eigenvectors have been rotated and sorted accordingly to their sensitivity to the pseudodata.
- The new first eigenvectors are indeed the ones contributing the most to the uncertainty error bands of up and down valence quarks distributions.

Thank you!

PDFs prospectives

Each PDF set comes with its error estimation:

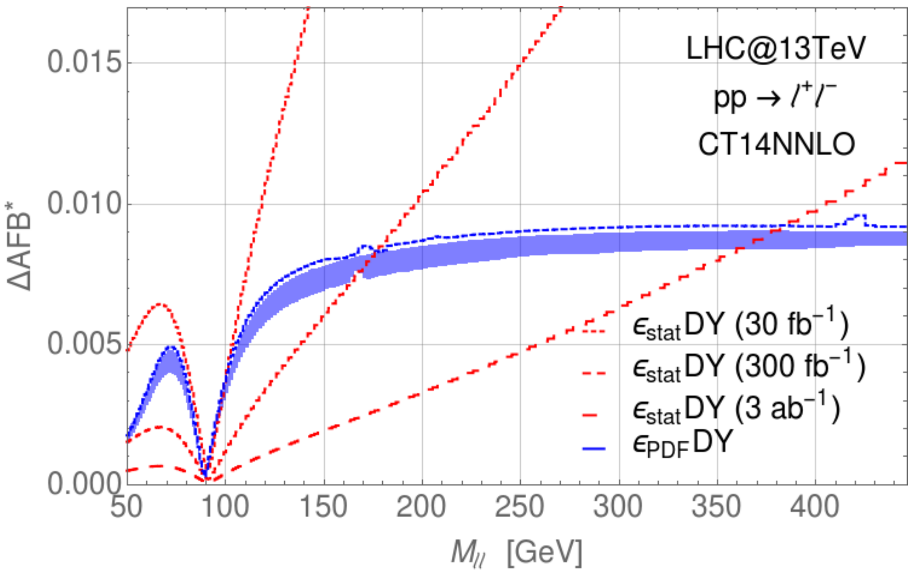

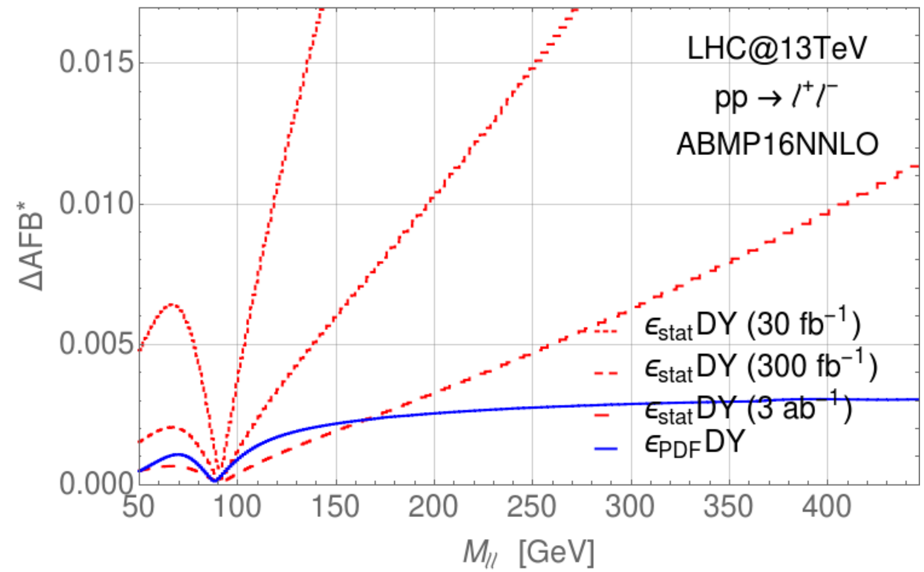

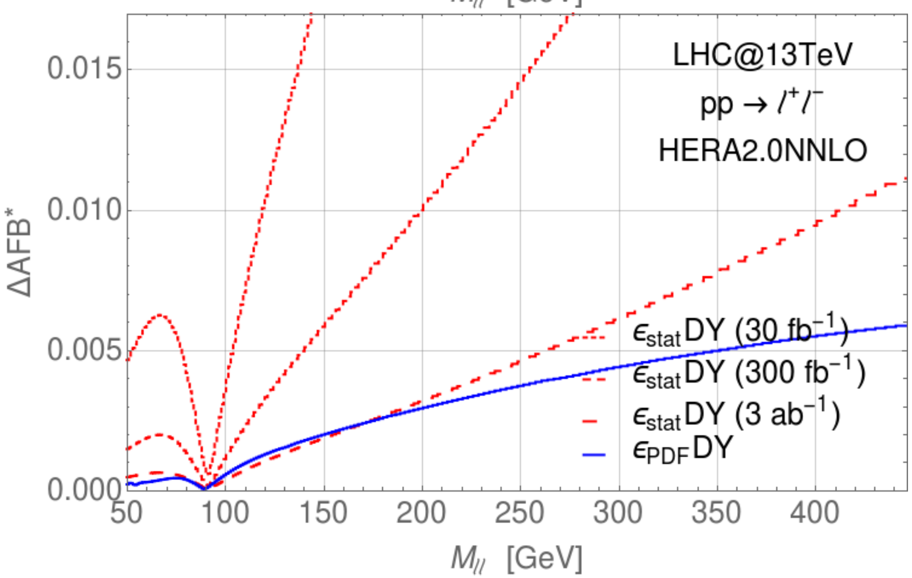

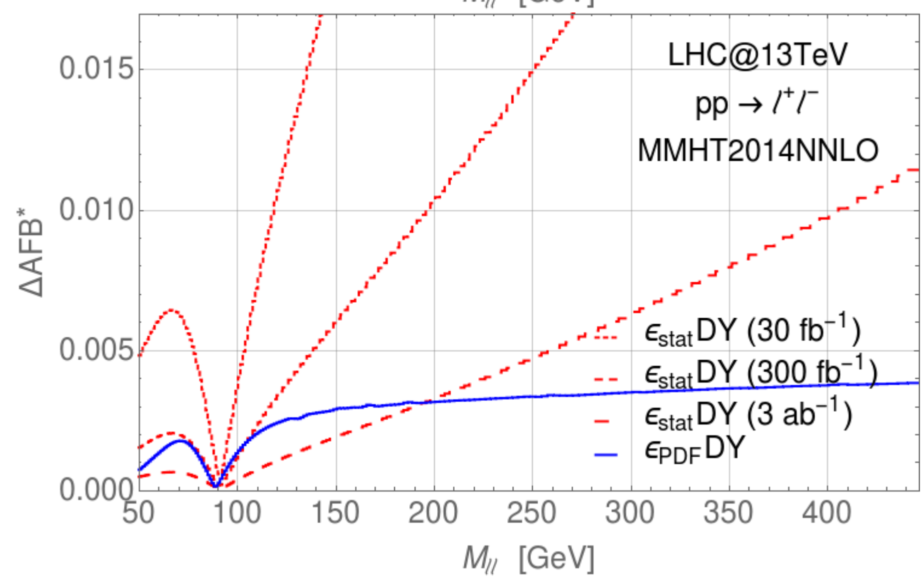

Each PDF fit would benefit from the inclusion of the AFB*.

Backup

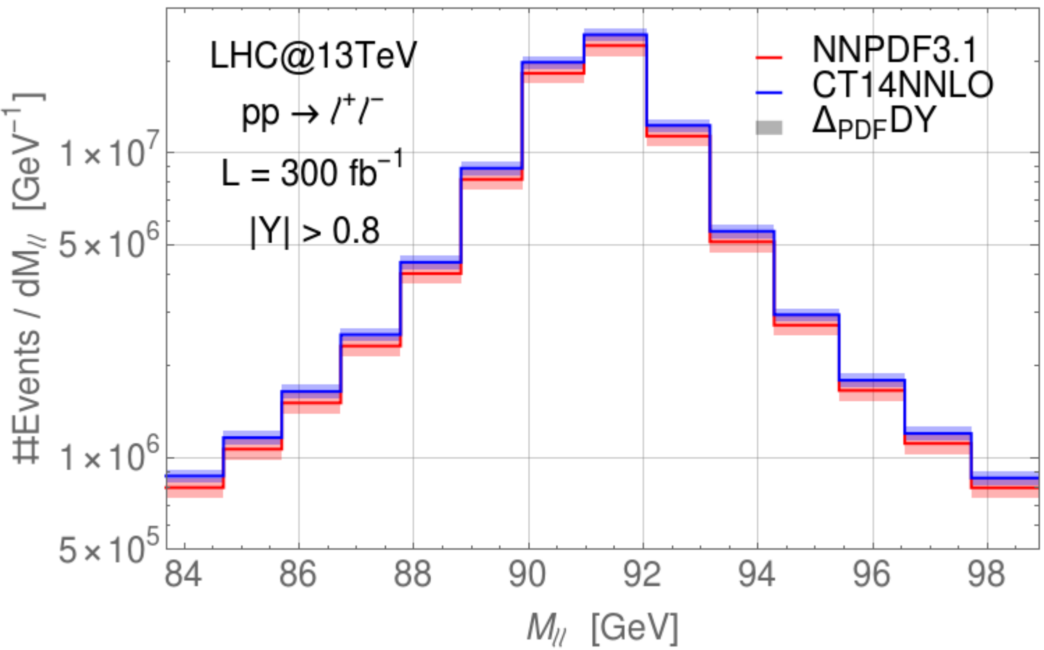
LHC@13TeV
pp → l^+l^-
L = 300 fb^{-1}
|Y| > 0.8
NNPDF3.1
CT14NNLO
Δ_{PDF}DY
#Events / dM$_{ll}$ [GeV^{-1}]
M_{ll} [GeV]

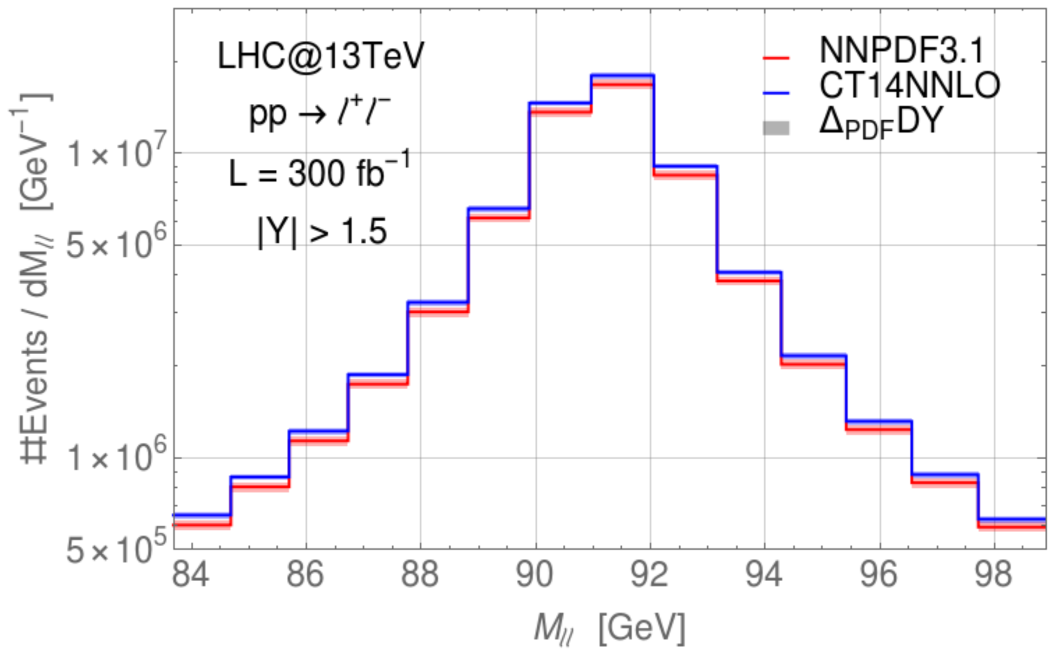
LHC@13TeV
pp → l^+l^-
L = 300 fb^{-1}
|Y| > 1.5
NNPDF3.1
CT14NNLO
Δ_{PDF}DY
#Events / dM$_{ll}$ [GeV^{-1}]
M_{ll} [GeV]

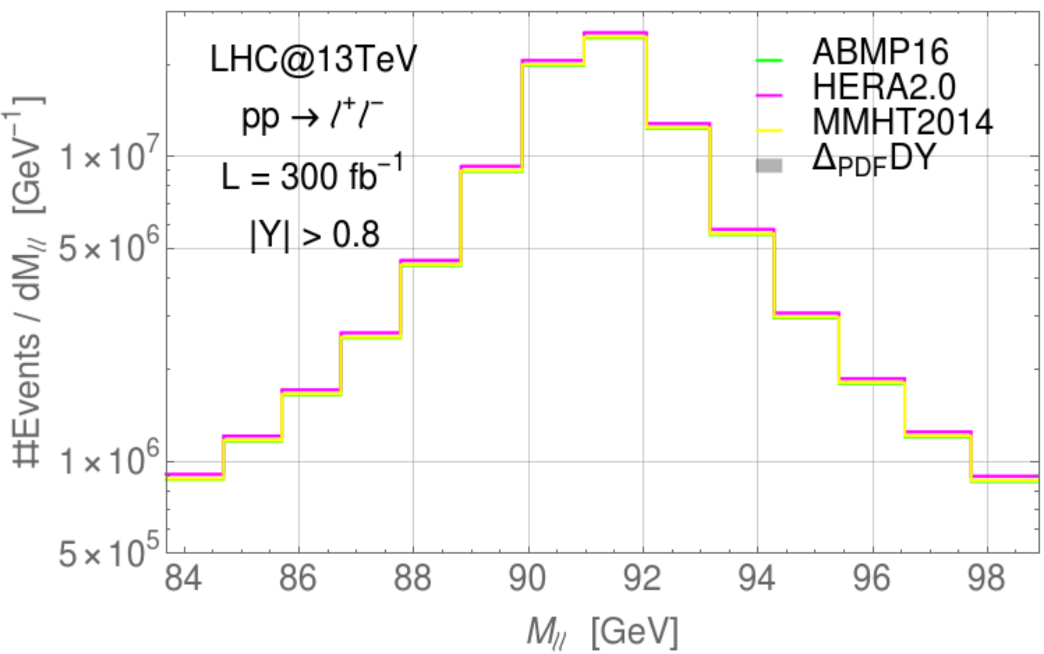
LHC@13TeV
pp → l^+l^-
L = 300 fb^{-1}
|Y| > 0.8
ABMP16
HERA2.0
MMHT2014
Δ_{PDF}DY
#Events / dM$_{ll}$ [GeV^{-1}]
M_{ll} [GeV]

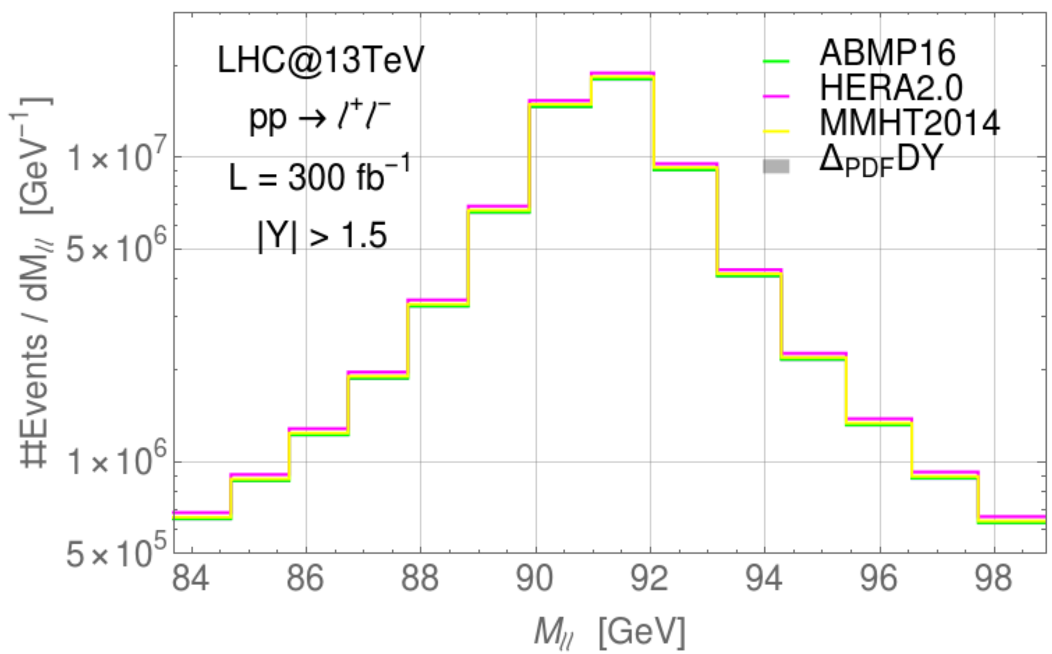
LHC@13TeV
pp → l^+l^-
L = 300 fb^{-1}
|Y| > 1.5
ABMP16
HERA2.0
MMHT2014
Δ_{PDF}DY
#Events / dM$_{ll}$ [GeV^{-1}]
M_{ll} [GeV]

Parton Luminosities

Imposing a high rapidity cut on the final state system we select processes arising from extreme Bjorken x regions.

With *|Y| = 4.5* at the *Z* pole we are exploring: $\begin{cases} x_1 \simeq 6\times10^{-1} \\ x_2 \simeq 8\times10^{-5} \end{cases}$ $\quad x_{1,2} = \frac{\sqrt{\hat{s}}}{\sqrt{s}}\, e^{\pm|Y|}$

(high-*x* valence quarks, low-*x* sea anti-quarks)

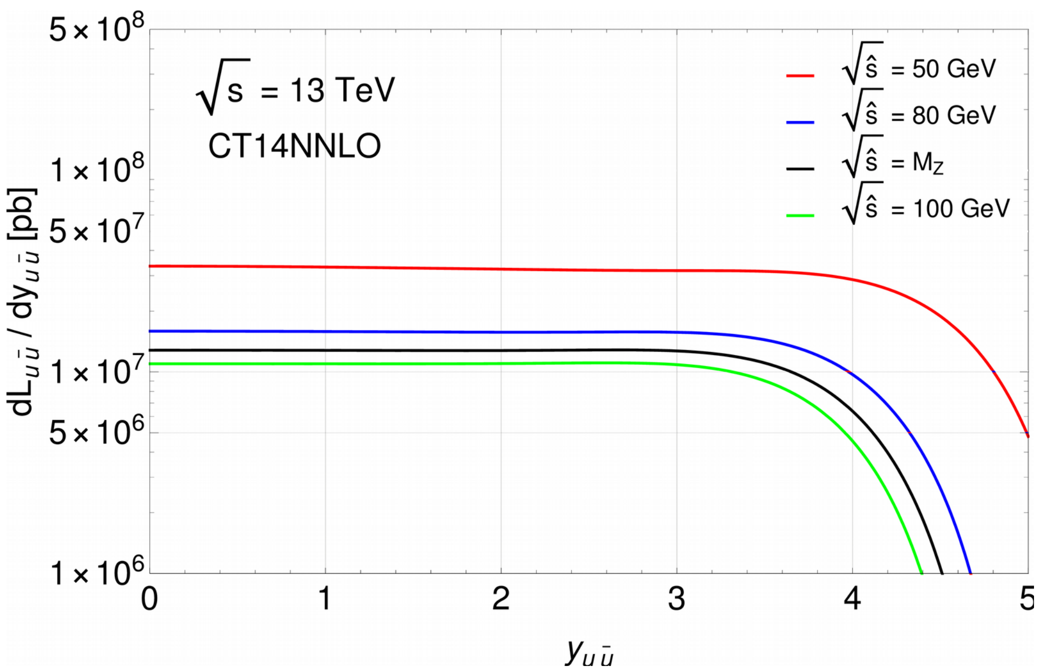

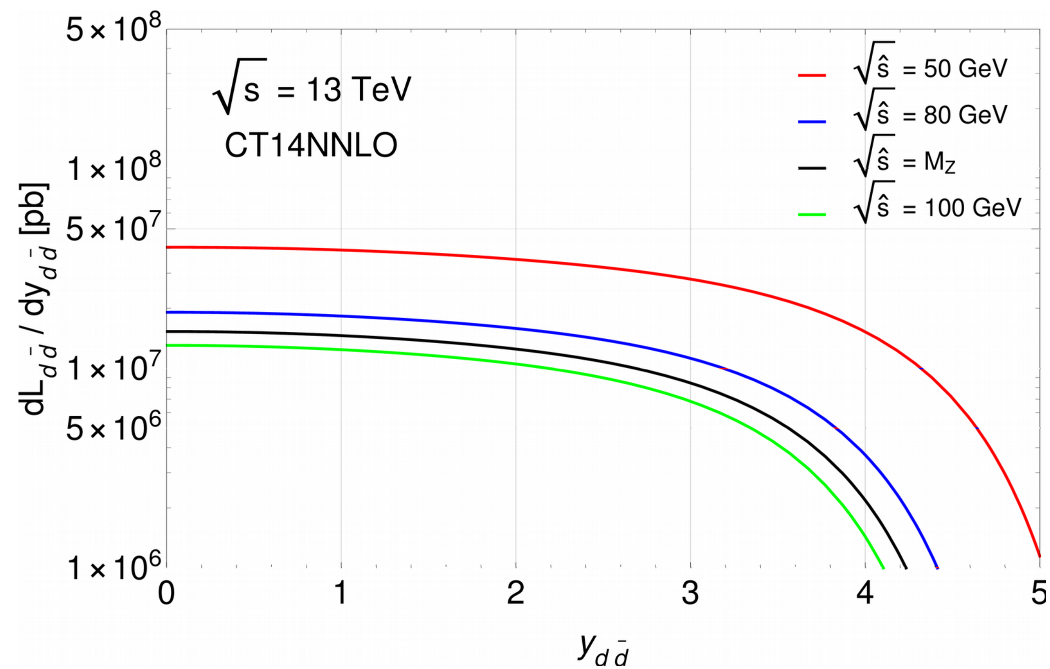

Processes initiated by $d\bar{d}$ interaction are more suppressed than $u\bar{u}$ initiated processes

Parton Luminosities Ratio

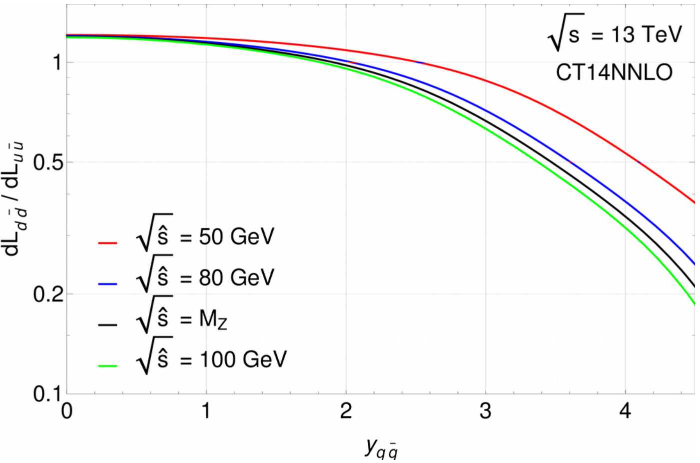

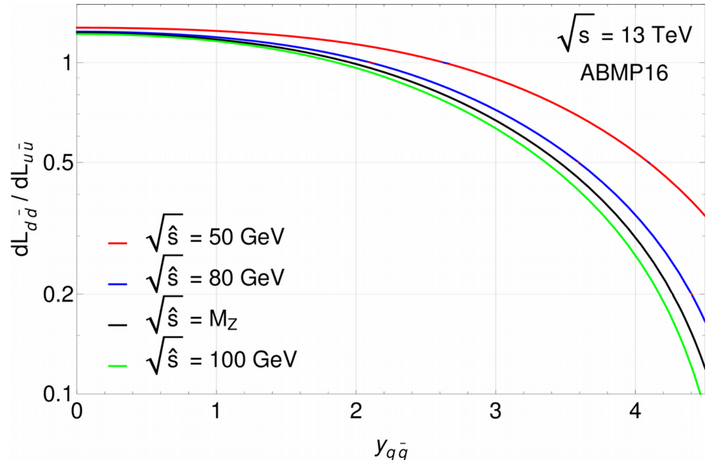

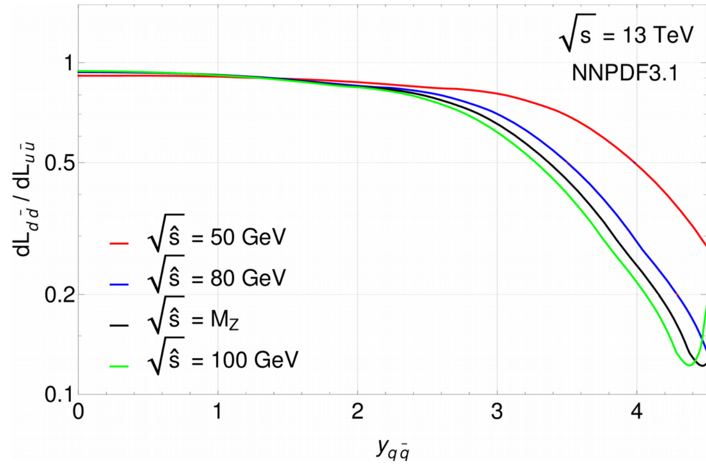

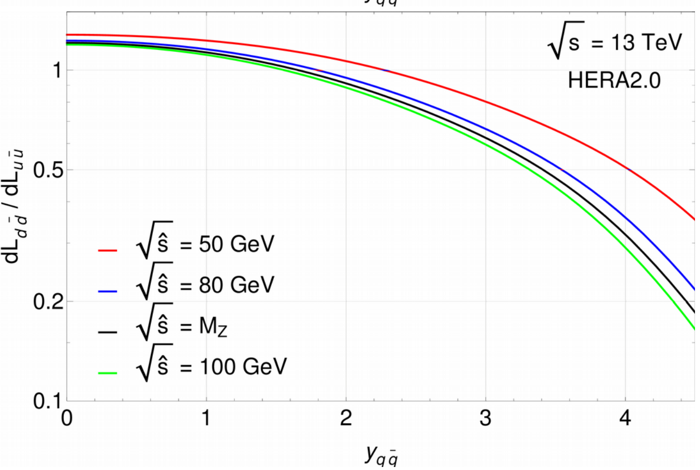

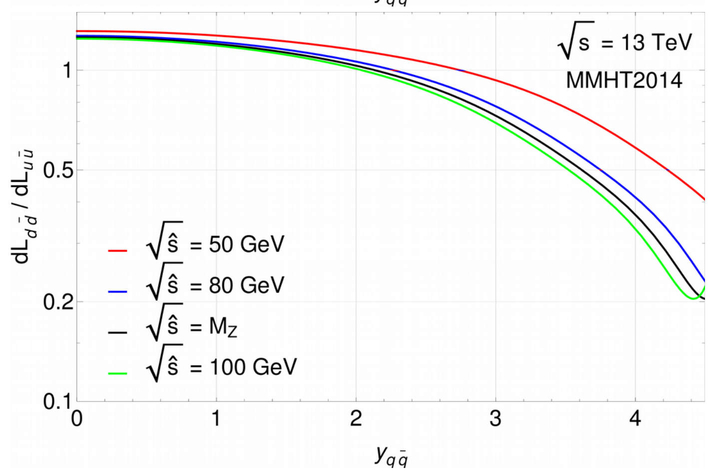

Each PDF set comes with its proper partonic content

A sufficiently high rapidity cut suppresses the contribution from $d\bar{d}$ interaction and gives us a direct handle on u and $\bar{u}$ PDFs.

Selecting *|Y| = 4.5* at the *Z* pole we have an overall contribution from $d\bar{d}$ initiated processes of:

CT14: 21%

ABMP: 12%

NNPDF: 12%

HERA: 18%

MMHT: 20%

Backup

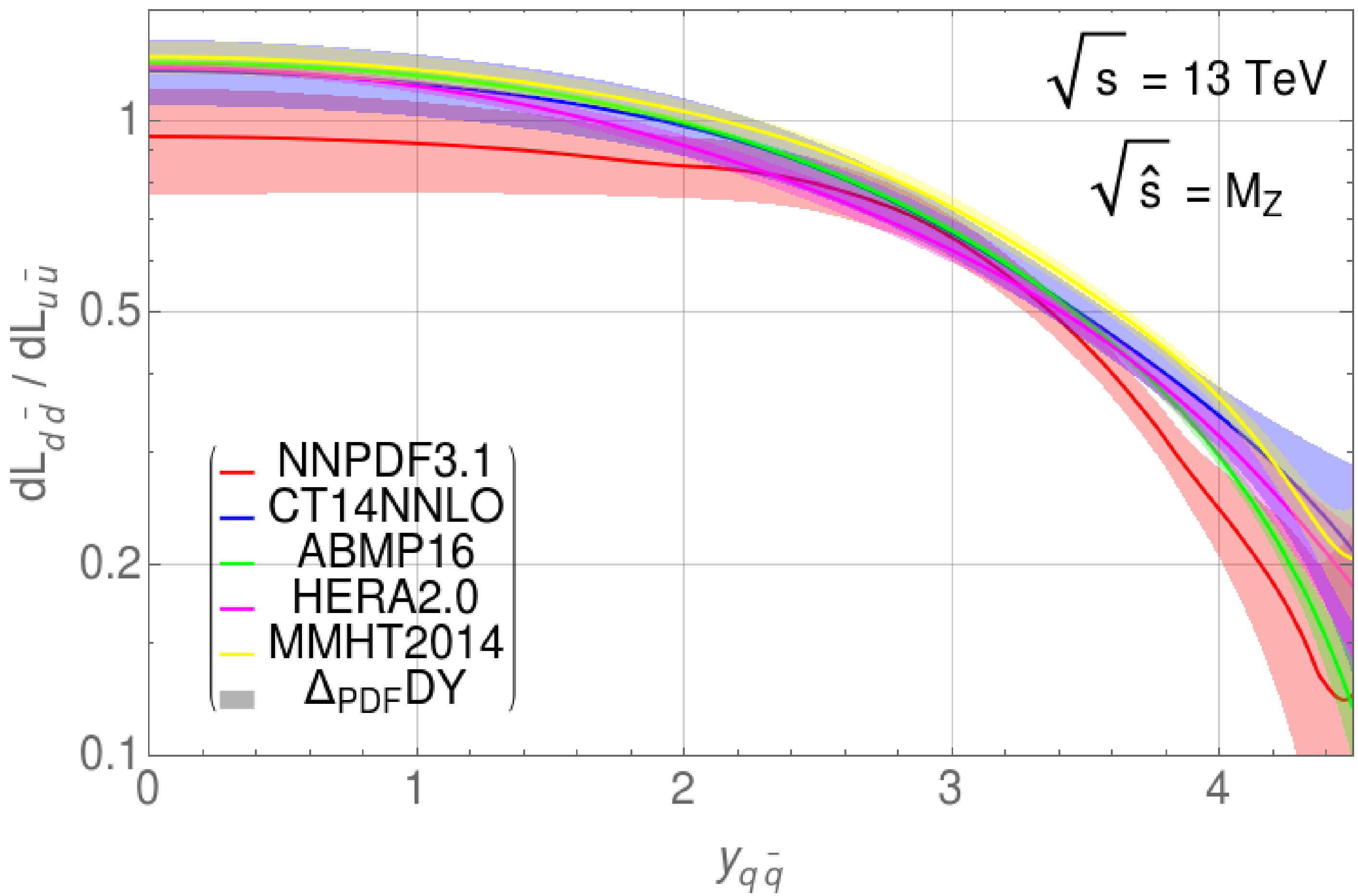

Selecting $|Y| = 4.5$ on the Z pole we have an overall contribution from $d\bar{d}$ initiated processes of:

NNPDF: 2% - 23% **CT14:** 13% - 29% **ABMP:** 10% - 14% **HERA:** 14% - 23% **MMHT:** 16% - 25%

Forward / Backward

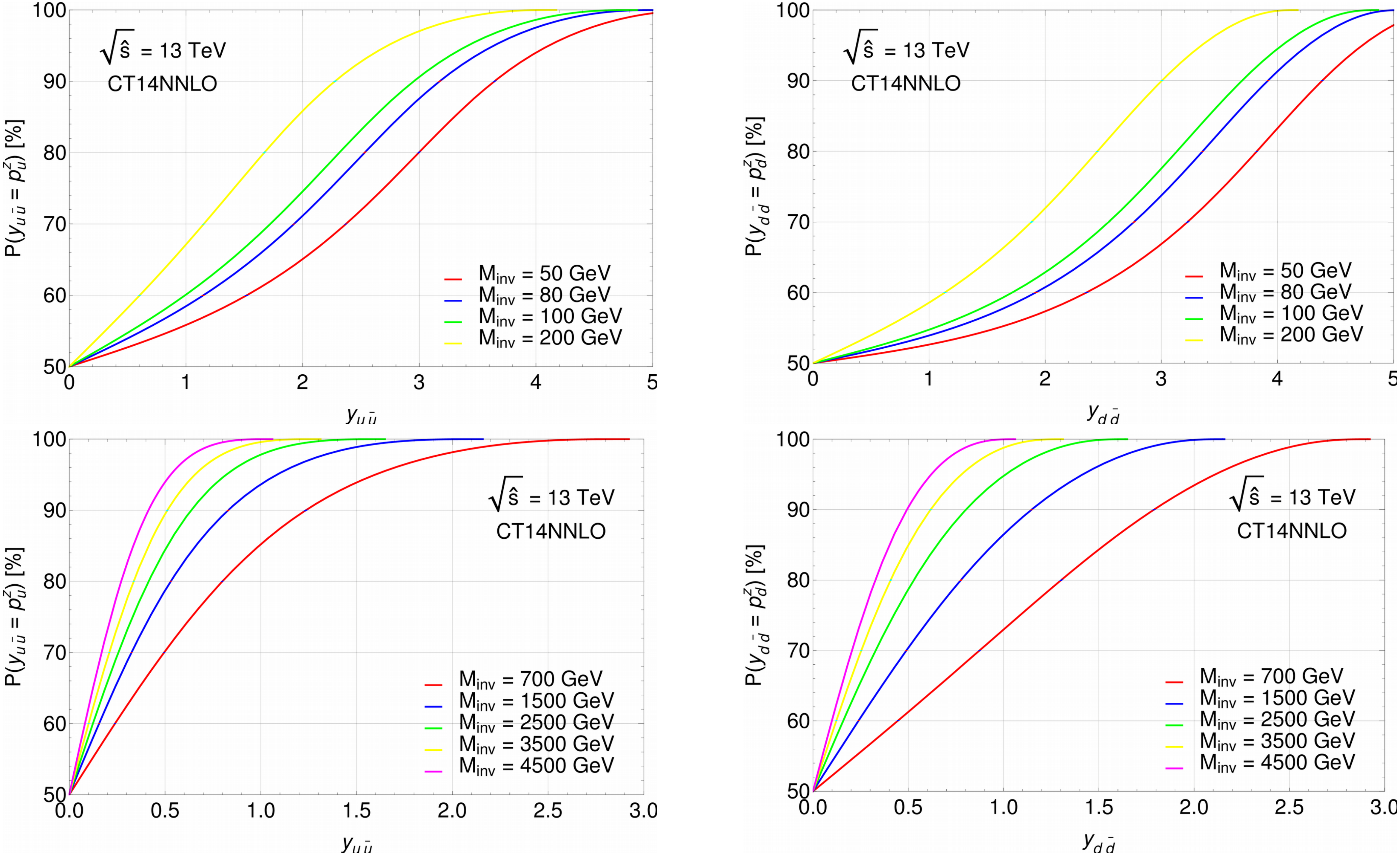

The probability of the direction of the boost matching the direction of the incoming quark grows with the rapidity cut and with the invariant mass, and it is higher for the *up* quarks

High rapidity measurements

Enhancing the rapidity cut we tend to the “true” AFB.

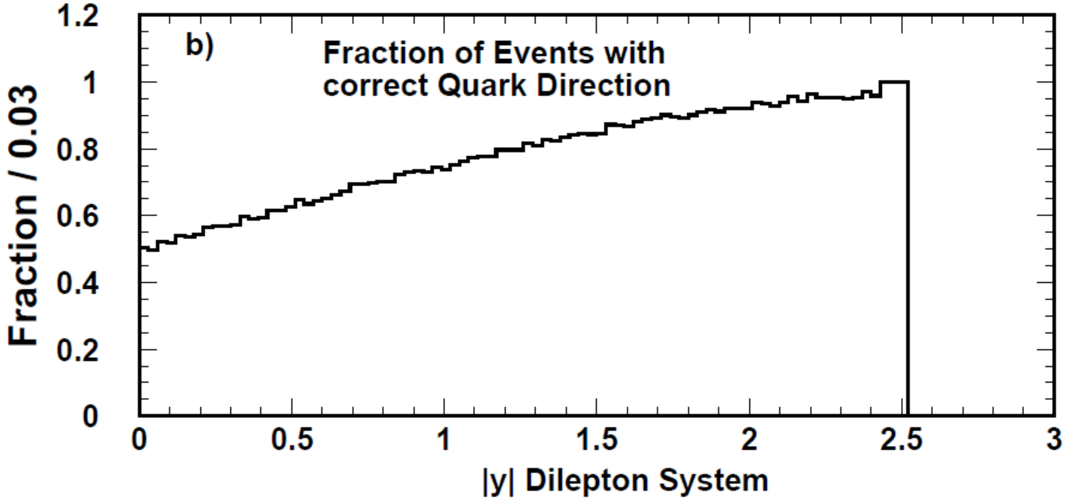

M. Dittmar, Phys.Rev.D55:161-166 (1997)

We are more likely to pick up the direction of the incoming quark (more energetic than the anti-quark).

The partonic luminosity of the down quarks is suppressed.

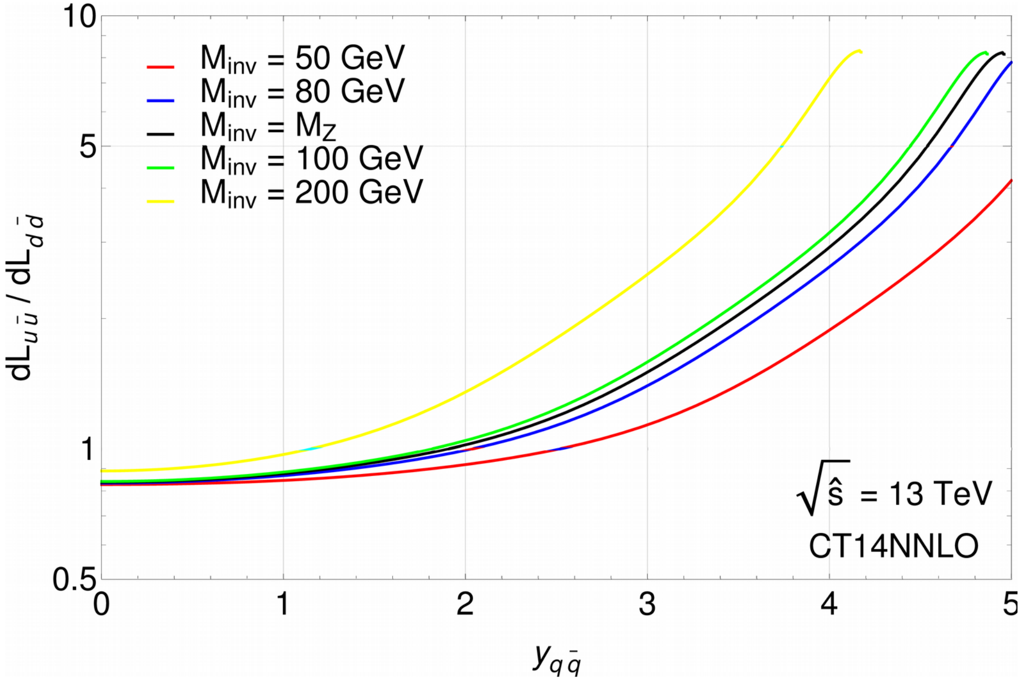

The AFB* in the high rapidity limit is produced by the $u\bar{u}$ interaction.

For *|Y| > 4.5* the down quarks contribution to the AFB* is ~ 20% at the Z pole (CT14NNLO prediction).

We have a <u>direct observation</u> on the *up* quarks PDF in the high-*x* region and a on the *anti-up* quarks in the low-*x* region.

Comparing PDF sets

AFB* measurements can be used to distinguish between different PDFs parametrizations.

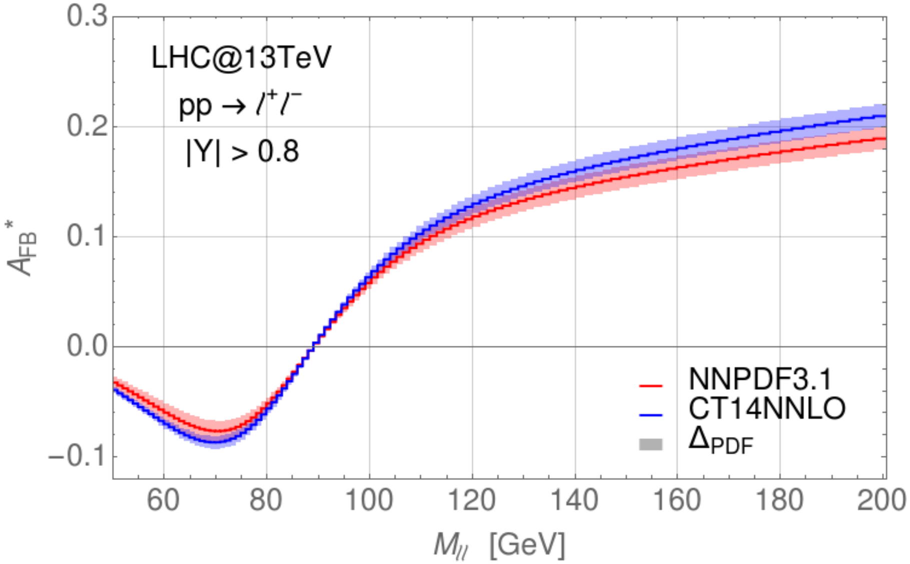

Statistics allows precise measurements

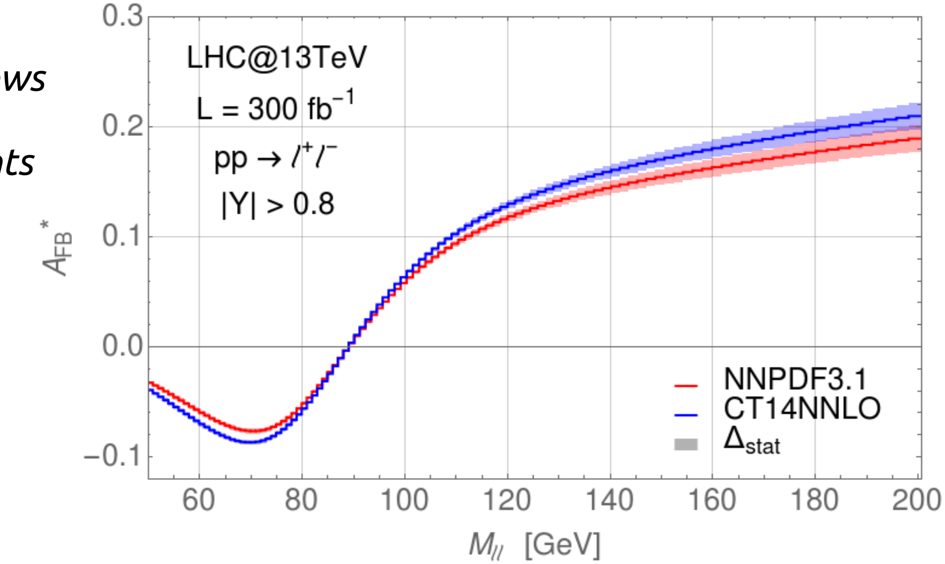

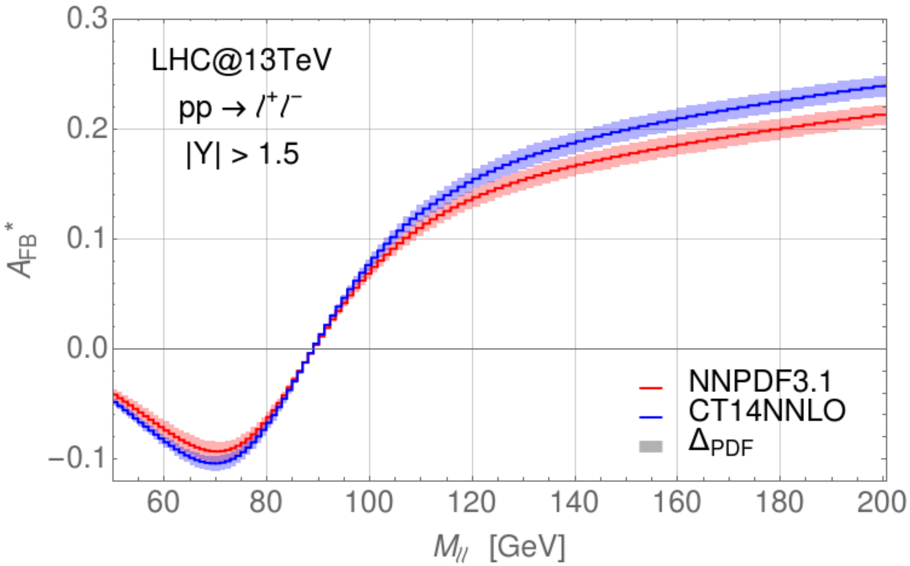

Systematics are under control

(and from what said before they can be further improved)

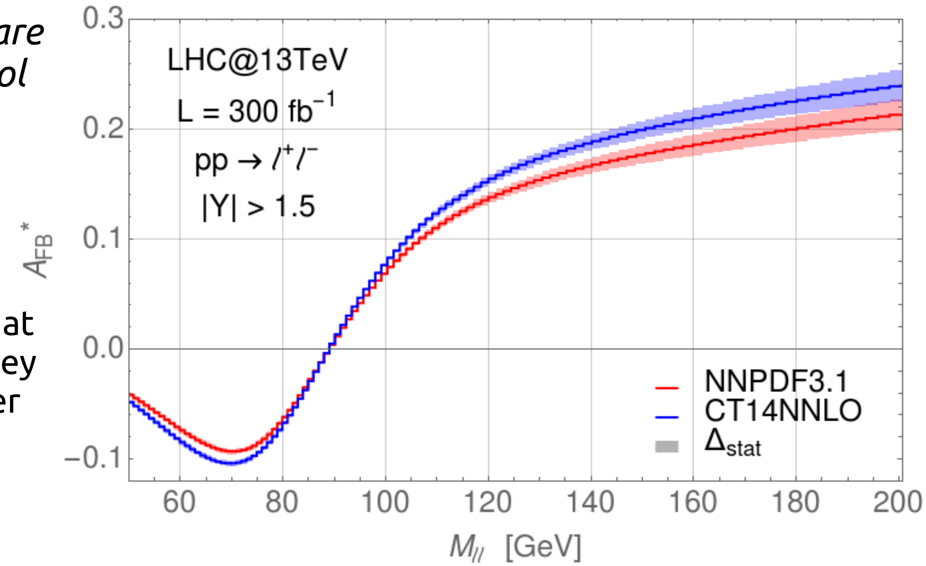

High rapidity cuts enhance the differences between PDF sets.

Comparing PDF sets

AFB* measurements can be used to distinguish between different PDFs parametrizations.

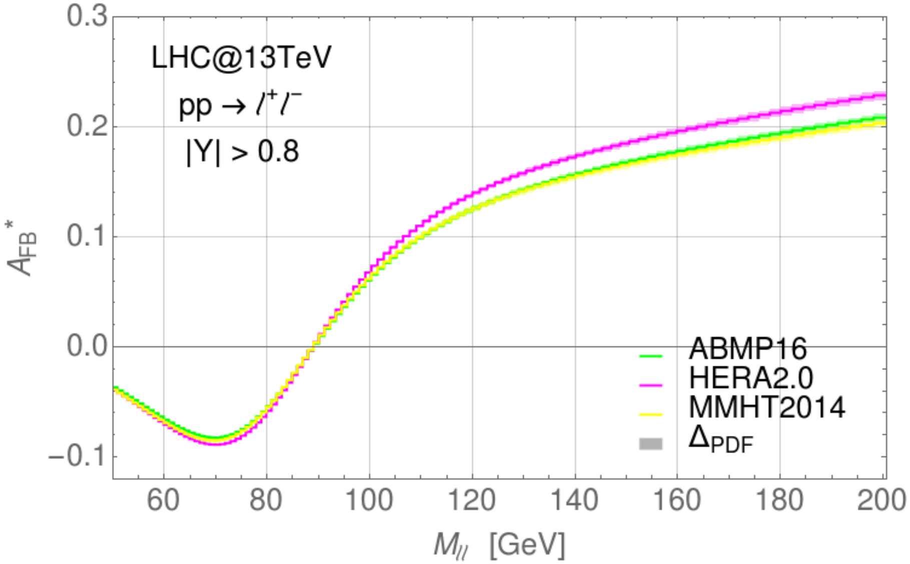

Statistics allows precise measurements

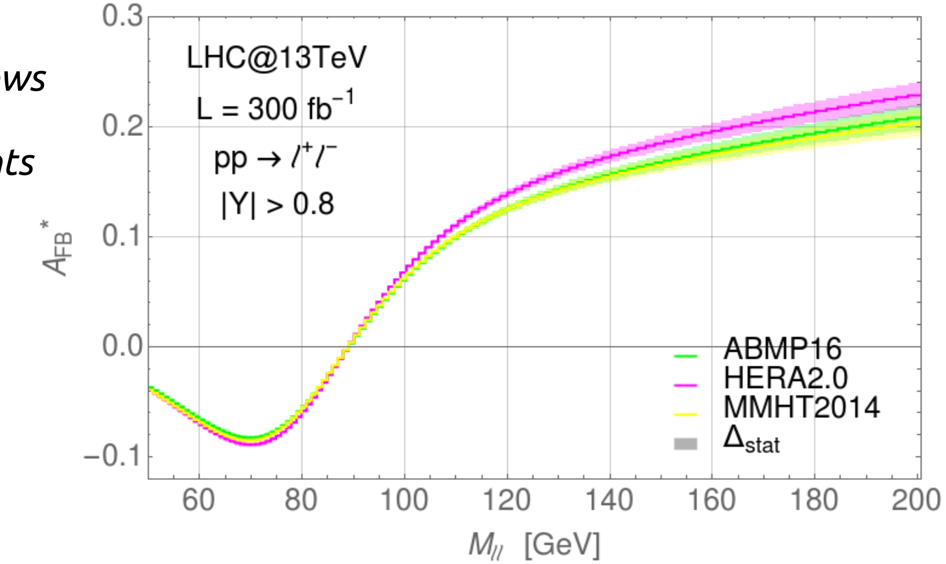

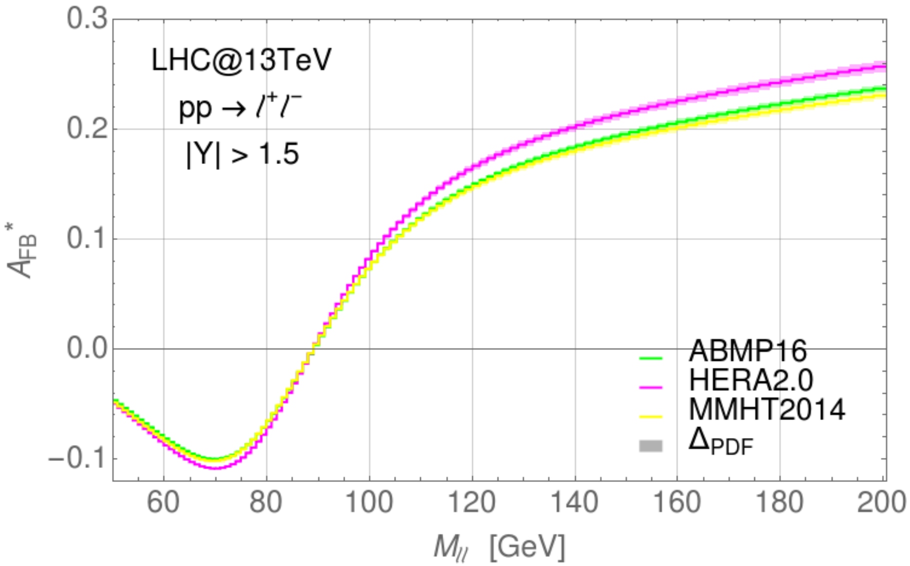

Systematics are under control

(and from what said before they can be further improved)

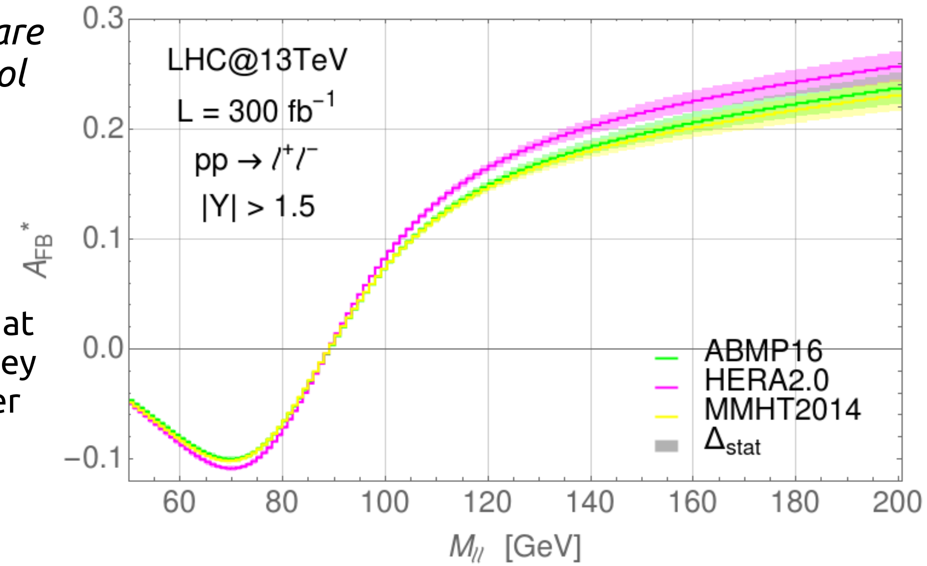

High rapidity cuts enhance the differences between PDF sets.

High rapidity cut

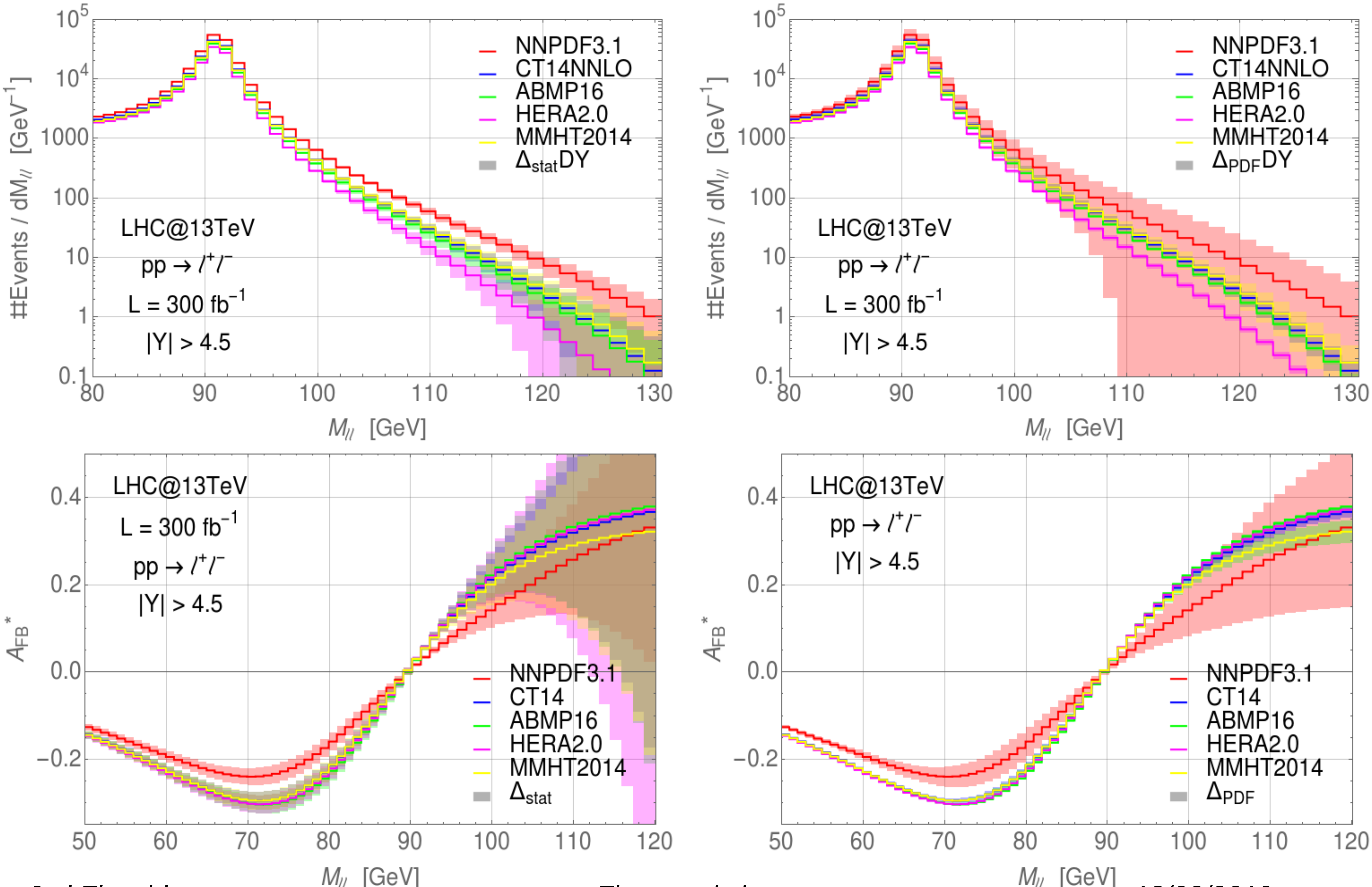

Backup

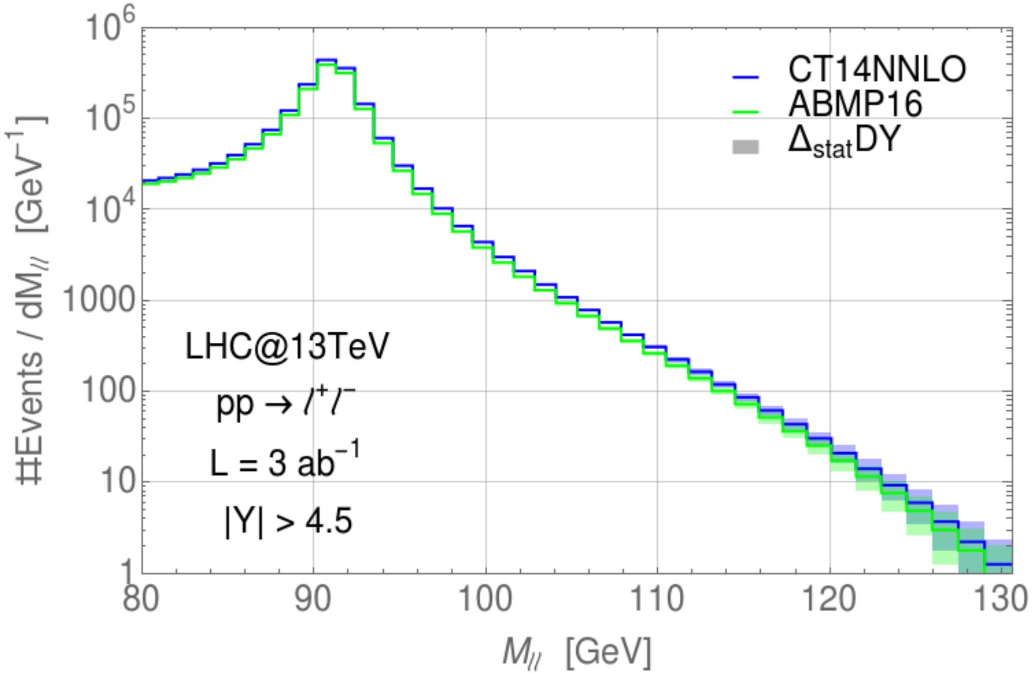
CT14NNLO
ABMP16
Δ_{stat}DY
LHC@13TeV
$pp \to l^+l^-$
$L = 3\ ab^{-1}$
$|Y| > 4.5$
#Events / dM_{ll} [GeV^{-1}]
M_{ll} [GeV]

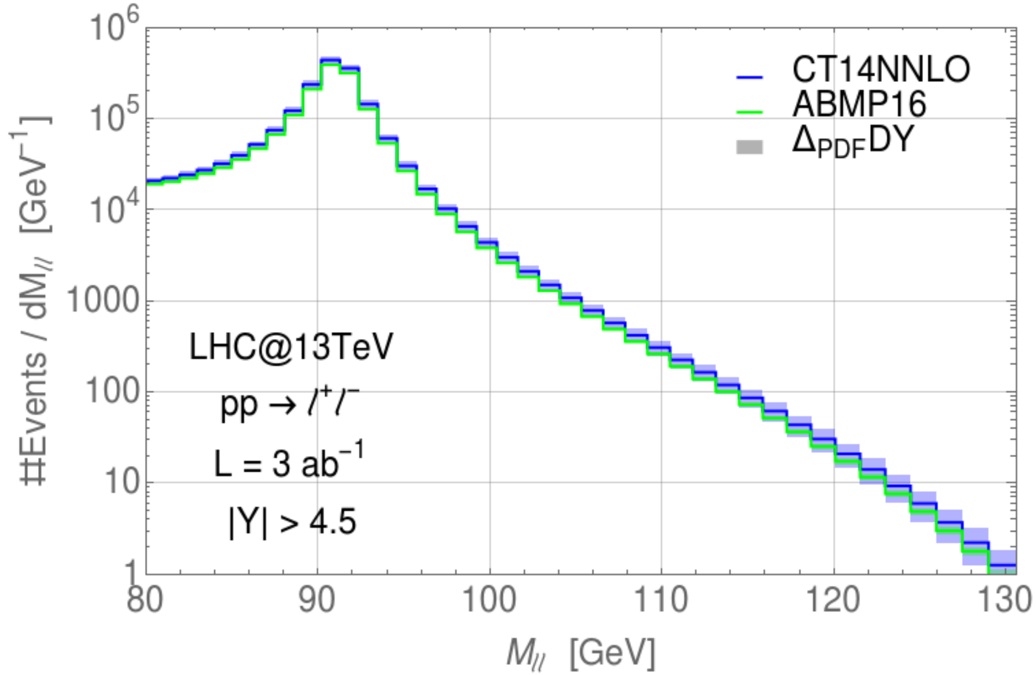
CT14NNLO
ABMP16
Δ_{PDF}DY
LHC@13TeV
$pp \to l^+l^-$
$L = 3\ ab^{-1}$
$|Y| > 4.5$
#Events / dM_{ll} [GeV^{-1}]
M_{ll} [GeV]

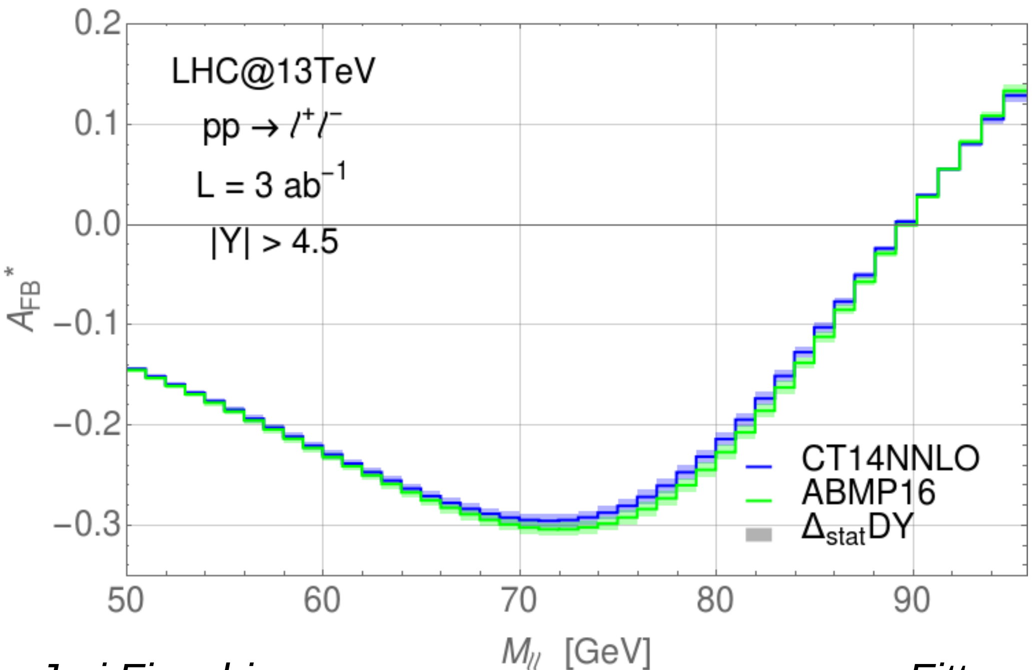
LHC@13TeV
$pp \to l^+l^-$
$L = 3\ ab^{-1}$
$|Y| > 4.5$
CT14NNLO
ABMP16
Δ_{stat}DY
A_{FB}^*
M_{ll} [GeV]

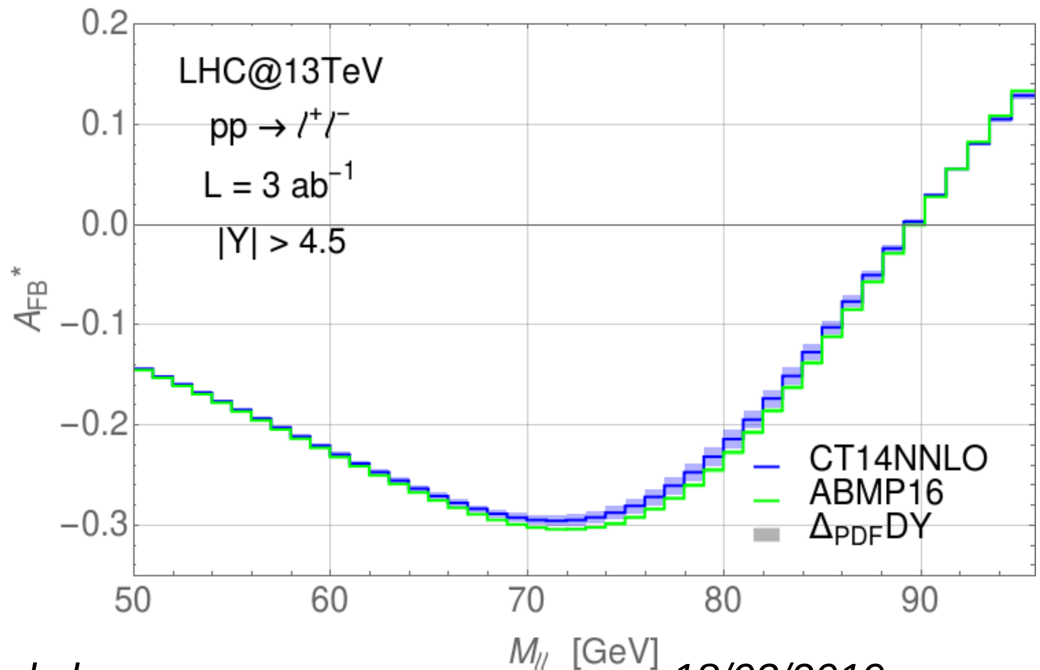
LHC@13TeV
$pp \to l^+l^-$
$L = 3\ ab^{-1}$
$|Y| > 4.5$
CT14NNLO
ABMP16
Δ_{PDF}DY
A_{FB}^*
M_{ll} [GeV]

Backup

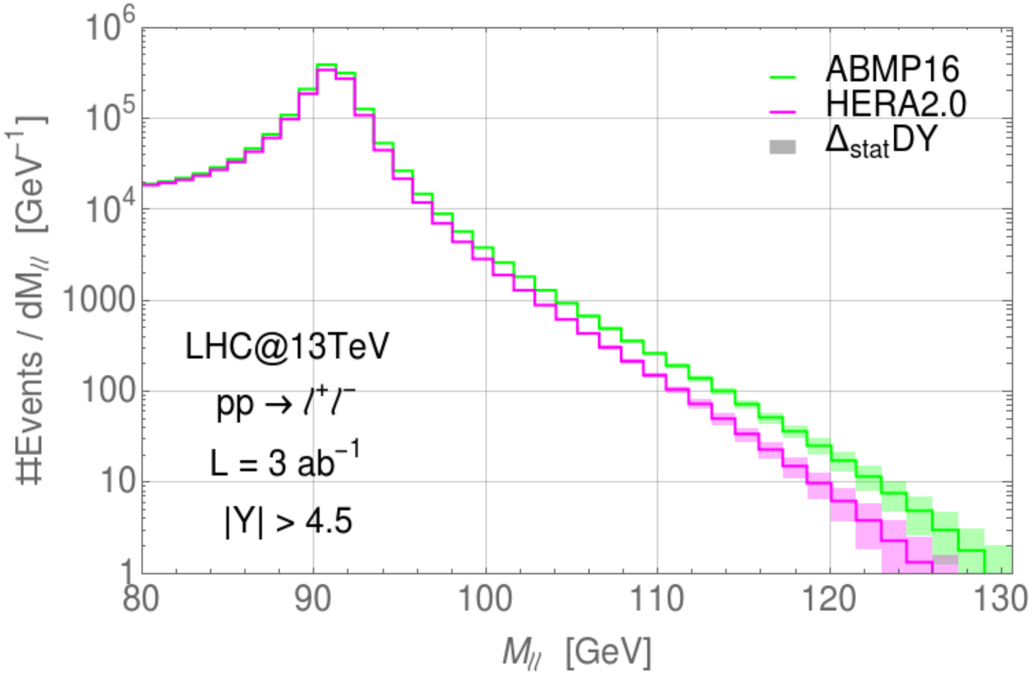

ABMP16
HERA2.0
Δ_{stat}DY
LHC@13TeV
$pp \to l^+l^-$
$L = 3\ ab^{-1}$
$|Y| > 4.5$
#Events / dM$_{ll}$ [GeV^{-1}]
M_{ll} [GeV]

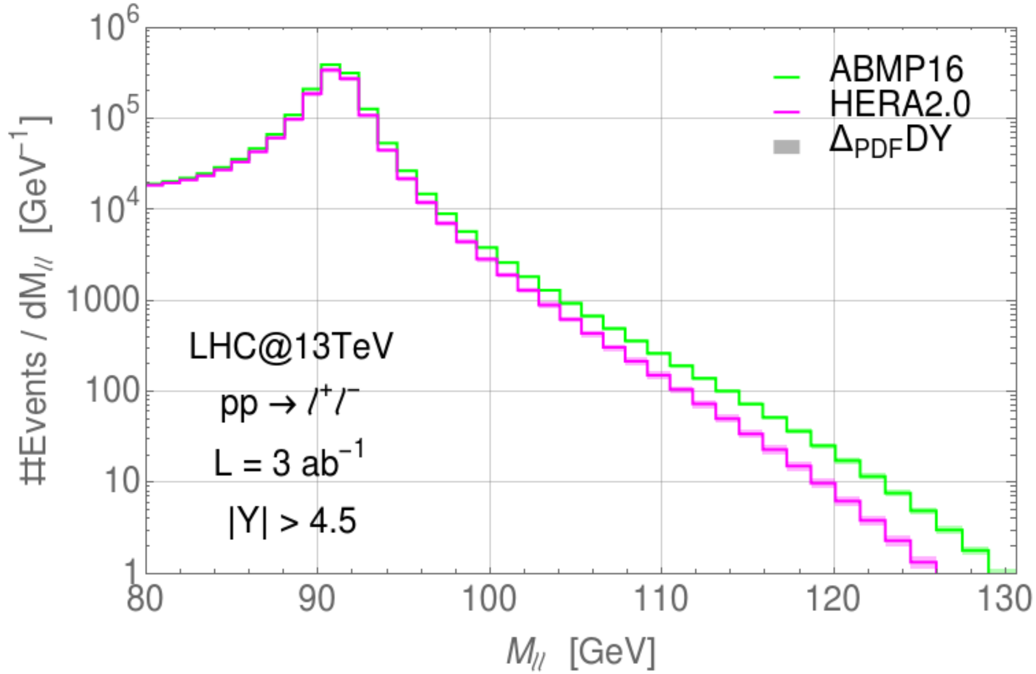

ABMP16
HERA2.0
Δ_{PDF}DY
LHC@13TeV
$pp \to l^+l^-$
$L = 3\ ab^{-1}$
$|Y| > 4.5$
#Events / dM$_{ll}$ [GeV^{-1}]
M_{ll} [GeV]

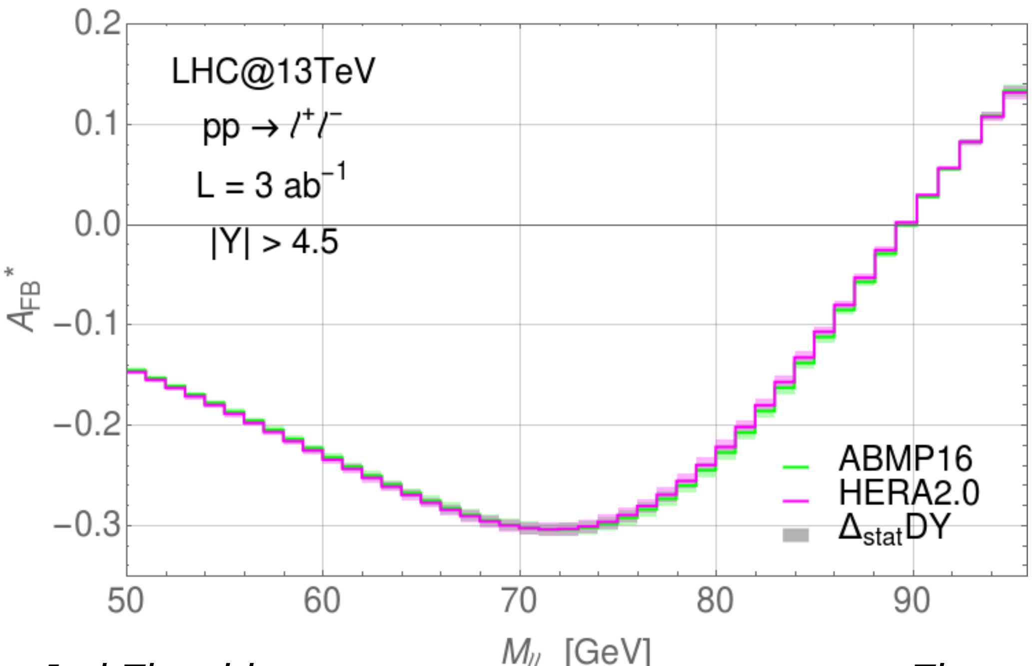

LHC@13TeV
$pp \to l^+l^-$
$L = 3\ ab^{-1}$
$|Y| > 4.5$
ABMP16
HERA2.0
Δ_{stat}DY
A_{FB}^*
M_{ll} [GeV]

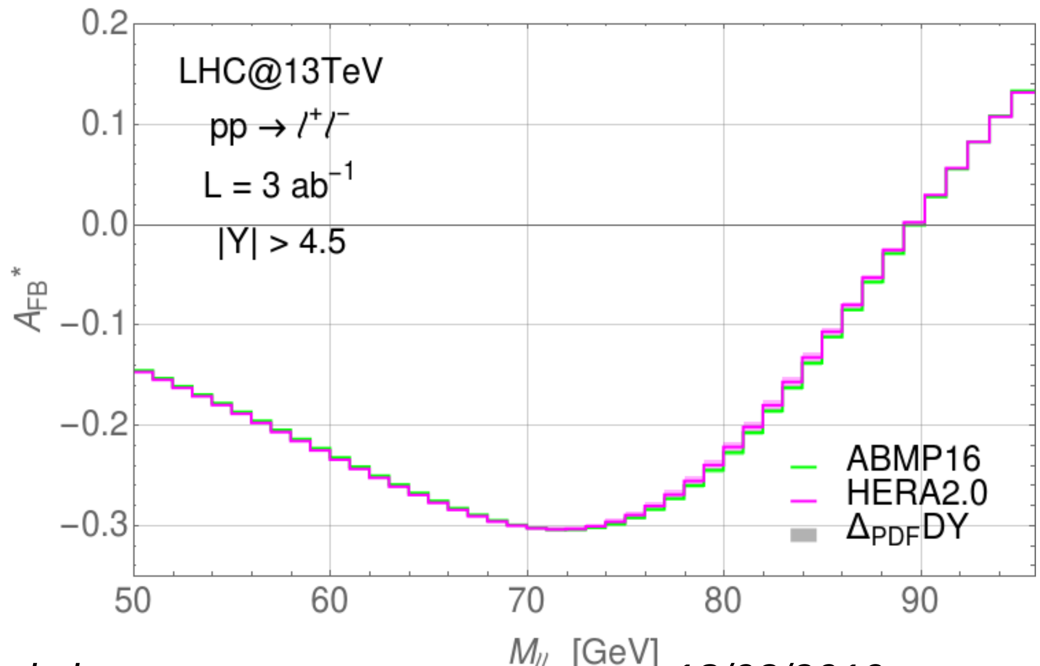

LHC@13TeV
$pp \to l^+l^-$
$L = 3\ ab^{-1}$
$|Y| > 4.5$
ABMP16
HERA2.0
Δ_{PDF}DY
A_{FB}^*
M_{ll} [GeV]

Backup

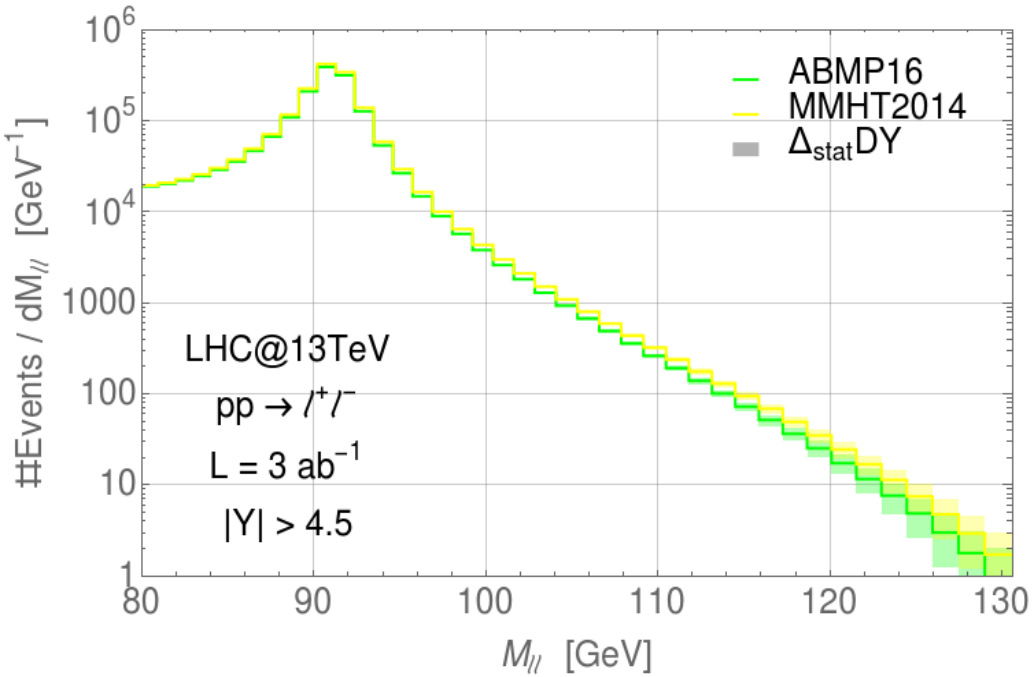
ABMP16
MMHT2014
Δ_{stat}DY
LHC@13TeV
pp → l^+l^-
L = 3 ab^{-1}
|Y| > 4.5
#Events / dM_{ll} [GeV^{-1}]
M_{ll} [GeV]

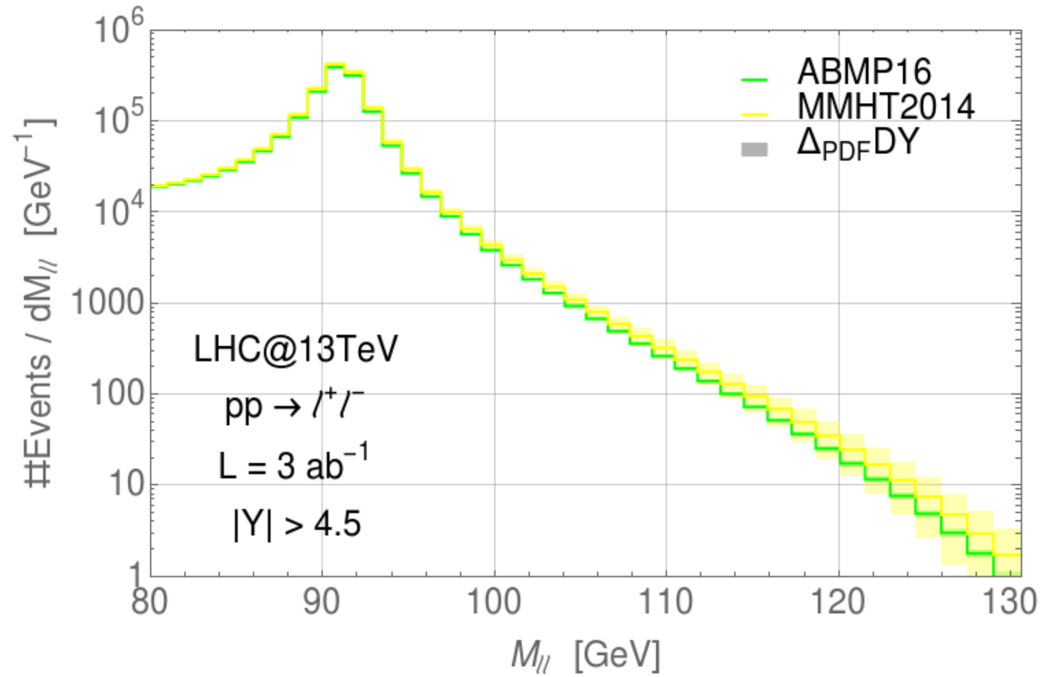
ABMP16
MMHT2014
Δ_{PDF}DY
LHC@13TeV
pp → l^+l^-
L = 3 ab^{-1}
|Y| > 4.5
#Events / dM_{ll} [GeV^{-1}]
M_{ll} [GeV]

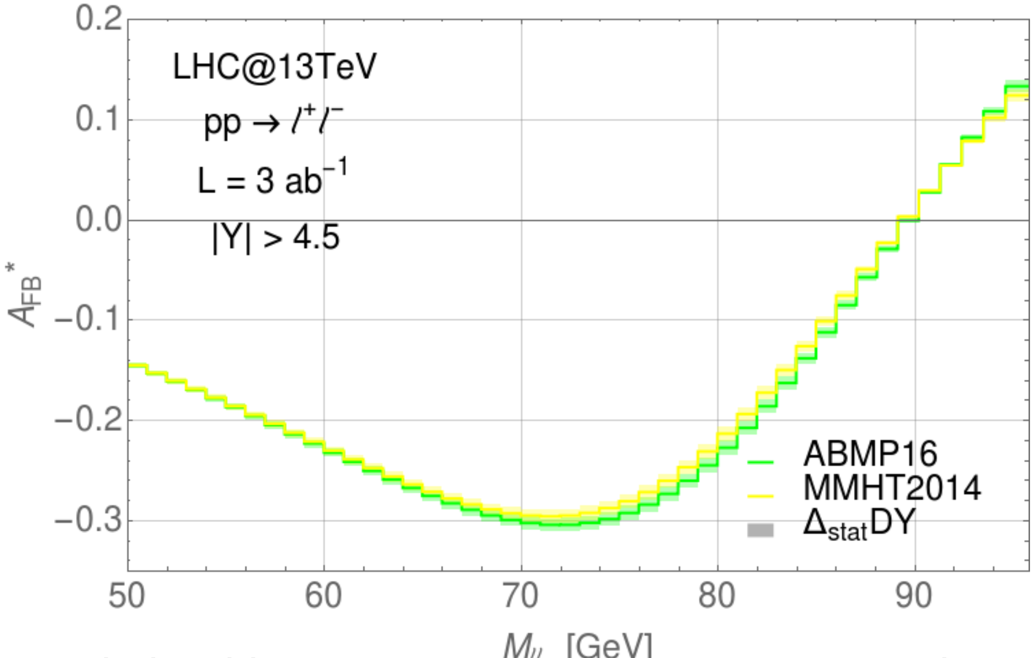
LHC@13TeV
pp → l^+l^-
L = 3 ab^{-1}
|Y| > 4.5
ABMP16
MMHT2014
Δ_{stat}DY
A_{FB}^*
M_{ll} [GeV]

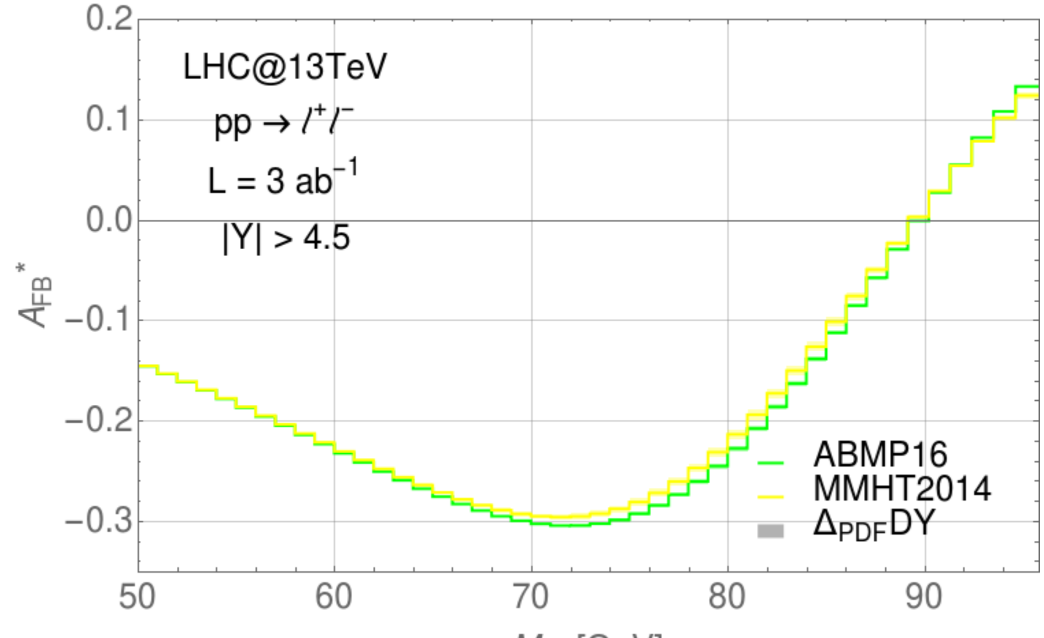
LHC@13TeV
pp → l^+l^-
L = 3 ab^{-1}
|Y| > 4.5
ABMP16
MMHT2014
Δ_{PDF}DY
A_{FB}^*
M_{ll} [GeV]

High rapidity measurements

Push to the limit: ***|Y| > 4.5***

(contribution of down quarks reduced to ~ 20%)

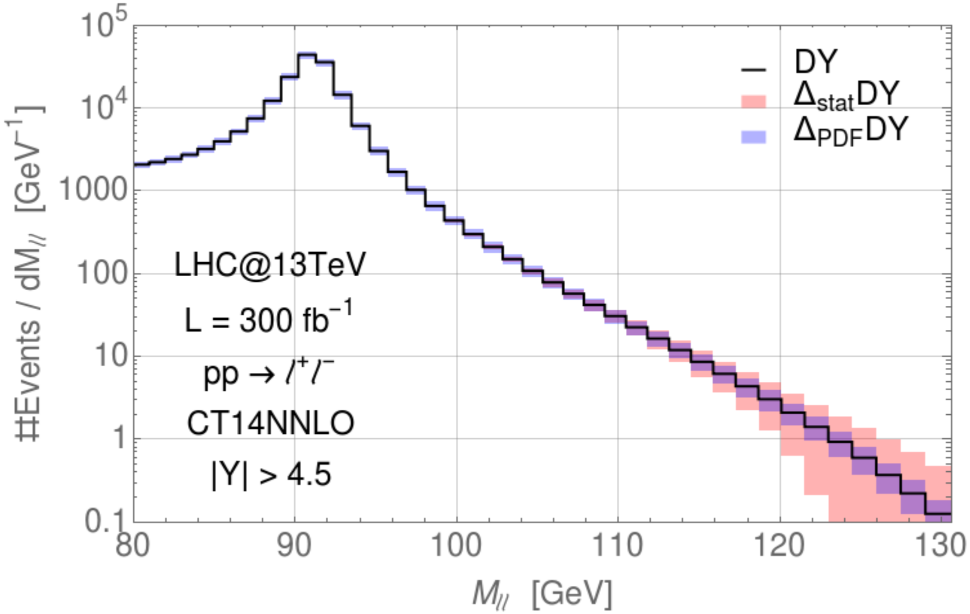

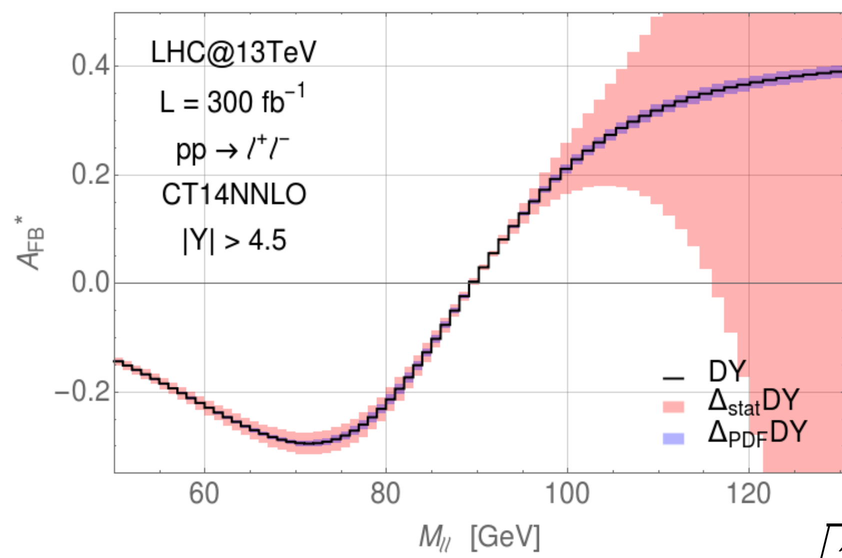

At the Z pole we are exploring:

$$\begin{cases} x_1 \simeq 6\times10^{-1} \\ x_2 \simeq 8\times10^{-5} \end{cases}$$

$$x_1 = \frac{\sqrt{\hat{s}}}{\sqrt{s}} e^{+|Y|}$$

$$x_2 = \frac{\sqrt{\hat{s}}}{\sqrt{s}} e^{-|Y|}$$

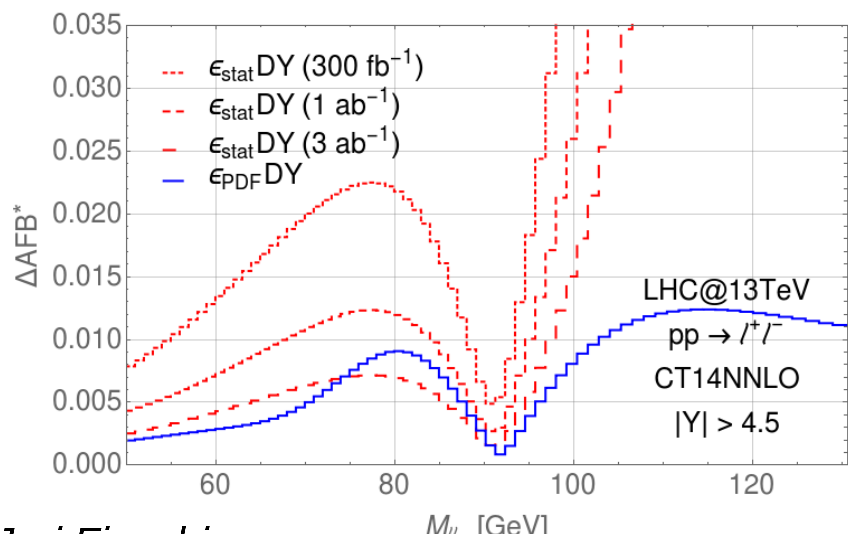

In the High-Luminosity stage we will have a sufficient statistic for the analysis.

AFB observable in xFitter

Implementation of ReactionAFB:

- Suited C++ code has been developed for the study of the sensitivity of PDF uncertainty on the reconstructed Forward-Backward Asymmetry data.

- Theory predictions for the observable are computed at LO.

- Parameters of the calculations added in the “.yaml” card for better flexibility.
  - Collider energy
  - Acceptance cuts
  - Rapidity cuts

- Integration routine from GSL library:
  - `integration : QAG`

    Adaptive Gauss-Kronrod integration with 61 point Gauss-Kronrod rule.
    - Analysis on one PDF eigenvector in about ~ 1 to 2 minutes.

- Source code uploaded on the gitlab repository in the xFitter “AFB” branch:

  https://gitlab.com/fitters/xfitter/tree/afb

PDF profiling

NNPDF3.1 nnlo ($Q^2 = M_Z^2$ GeV^2) ($L = 300\ fb^{-1}$)

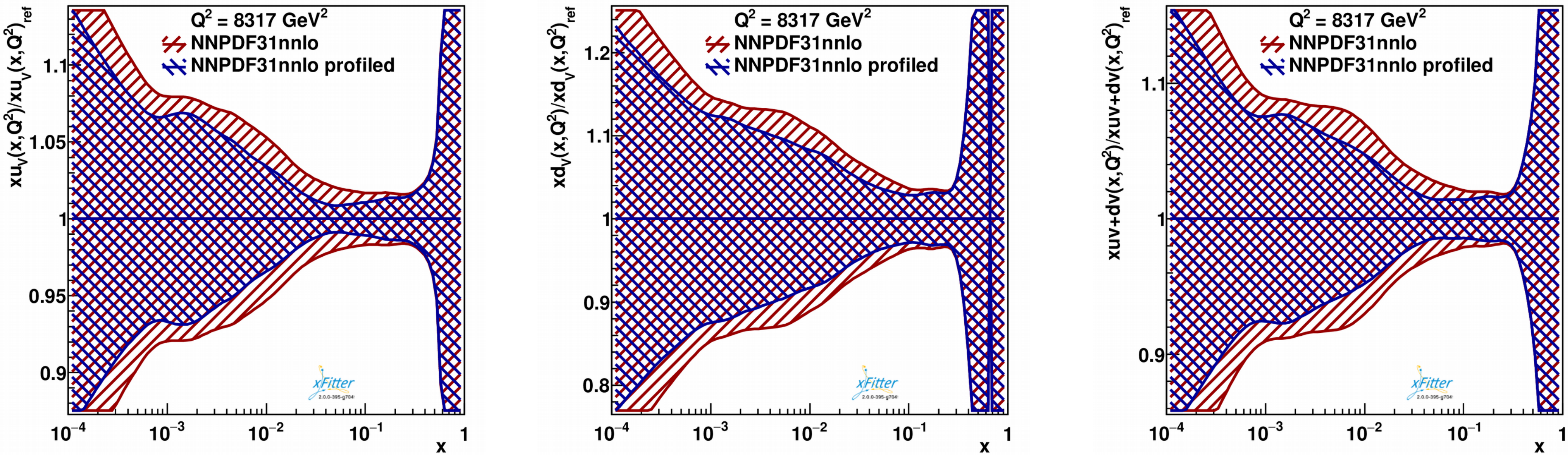

MMHT2014 nnlo ($Q^2 = M_Z^2$ GeV^2) ($L = 300\ fb^{-1}$)

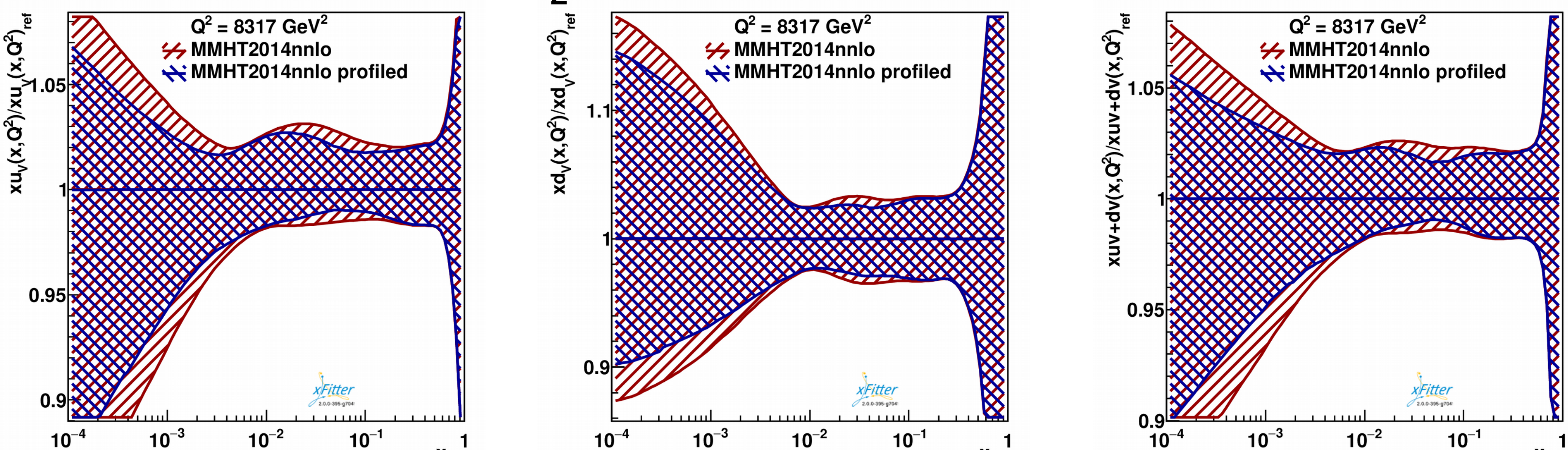

PDF profiling

ABMP16 nnlo ($Q^2 = M_Z^2$ GeV^2) (L = 300 fb^{-1})

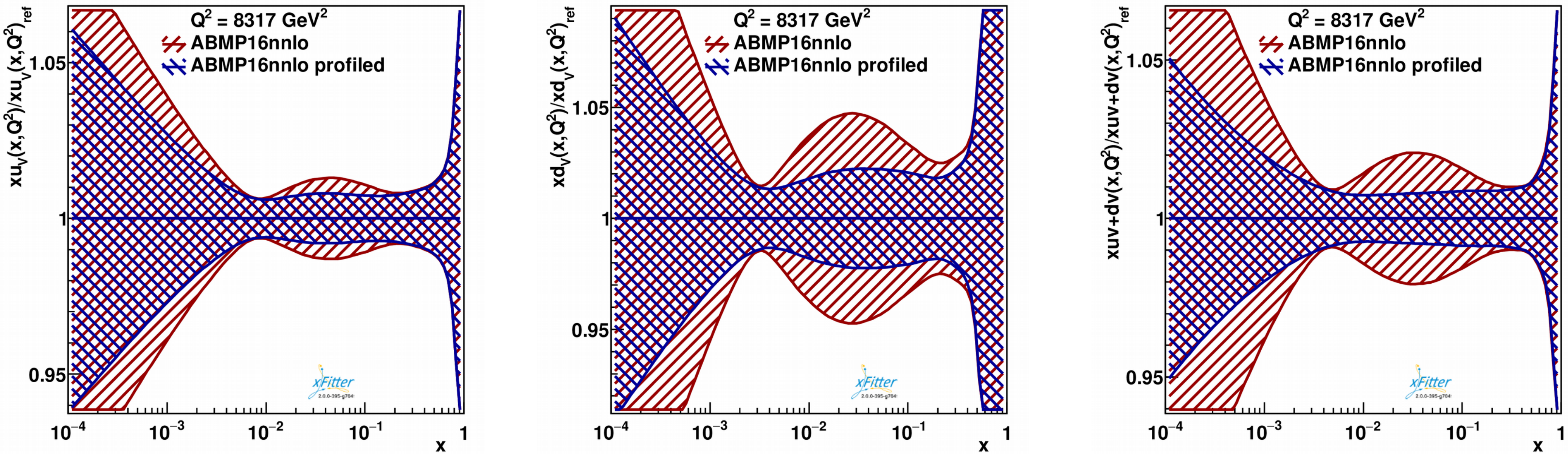

HERA2.0 nnlo ($Q^2 = M_Z^2$ GeV^2) (L = 300 fb^{-1})

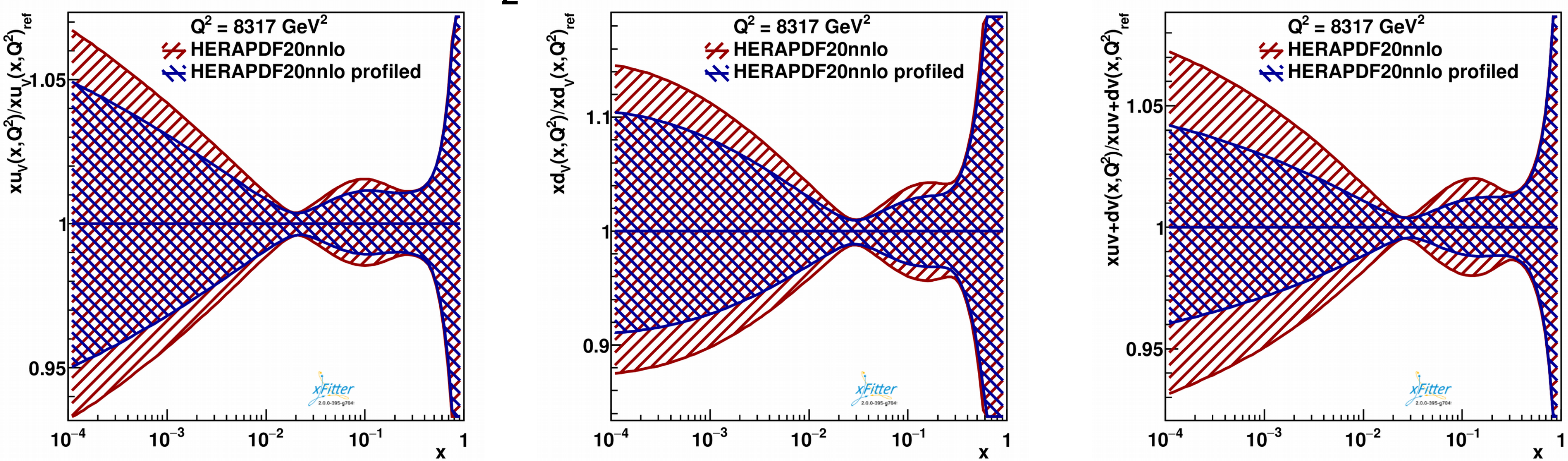

PDF profiling

CT14 nnlo ($Q^2 = M_Z^2$ GeV^2) ($L = 3000$ fb^{-1}) |Y| > 0 |Y| > 0.8

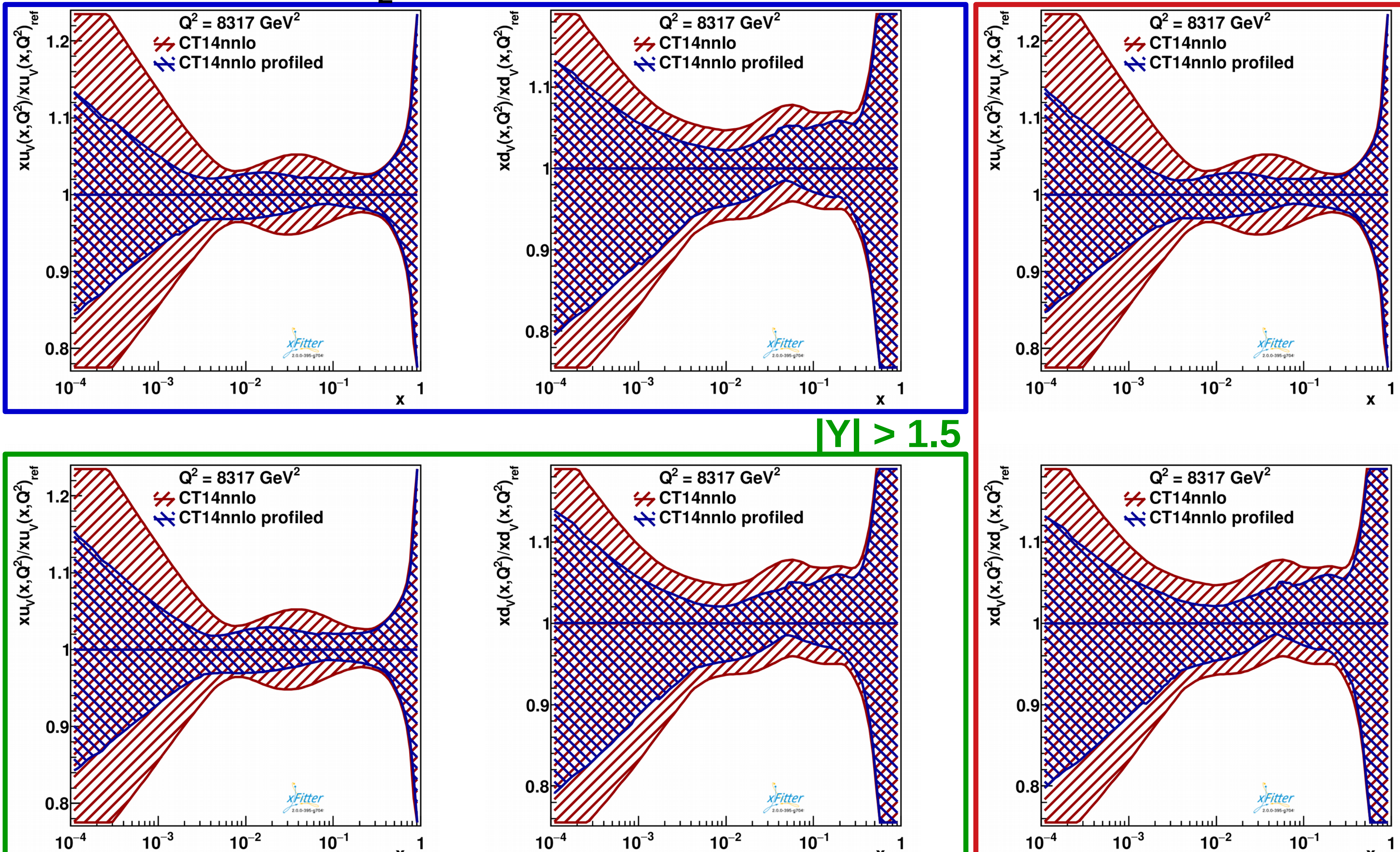

PDF profiling

ABMPnnlo ($Q^2 = M_Z^2$ GeV^2) ($L = 3000$ fb^{-1})

|Y| > 0

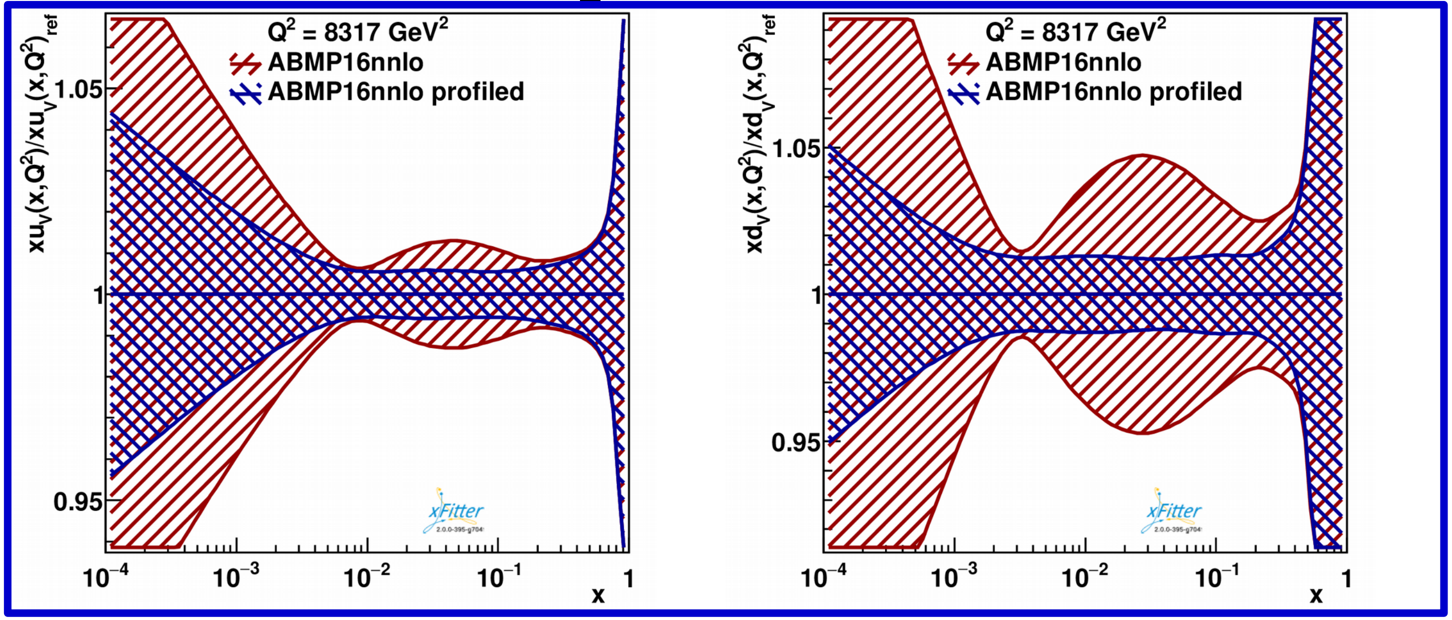

|Y| > 0.8

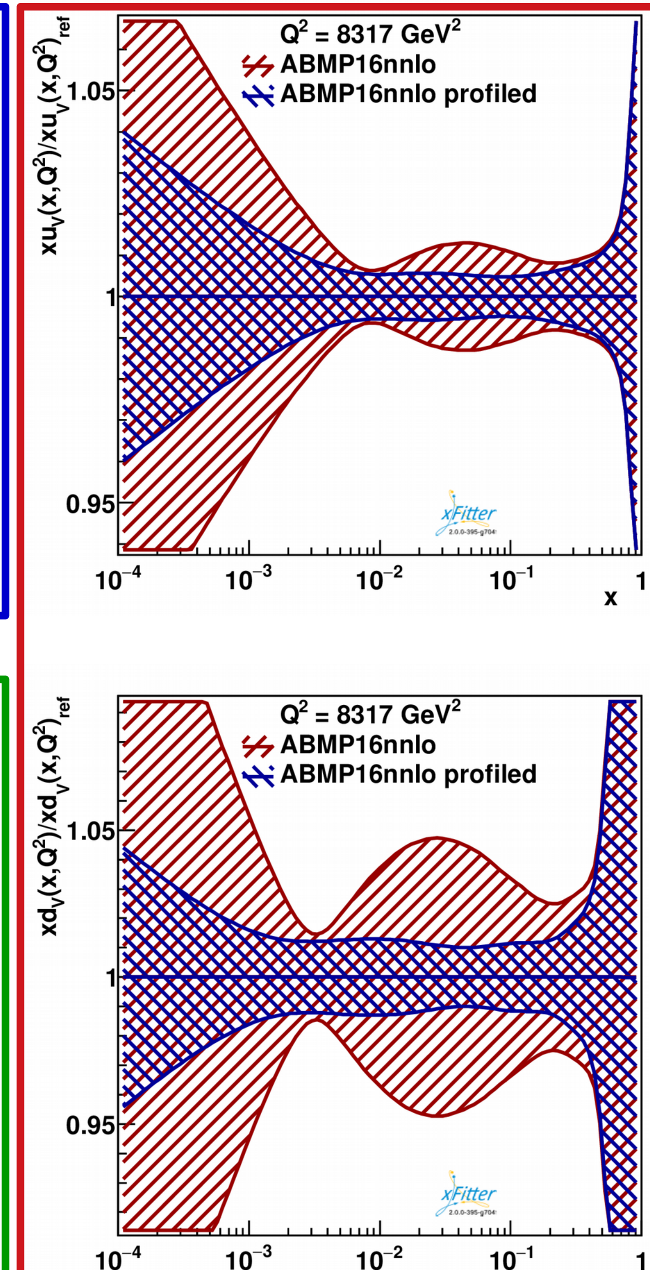

|Y| > 1.5

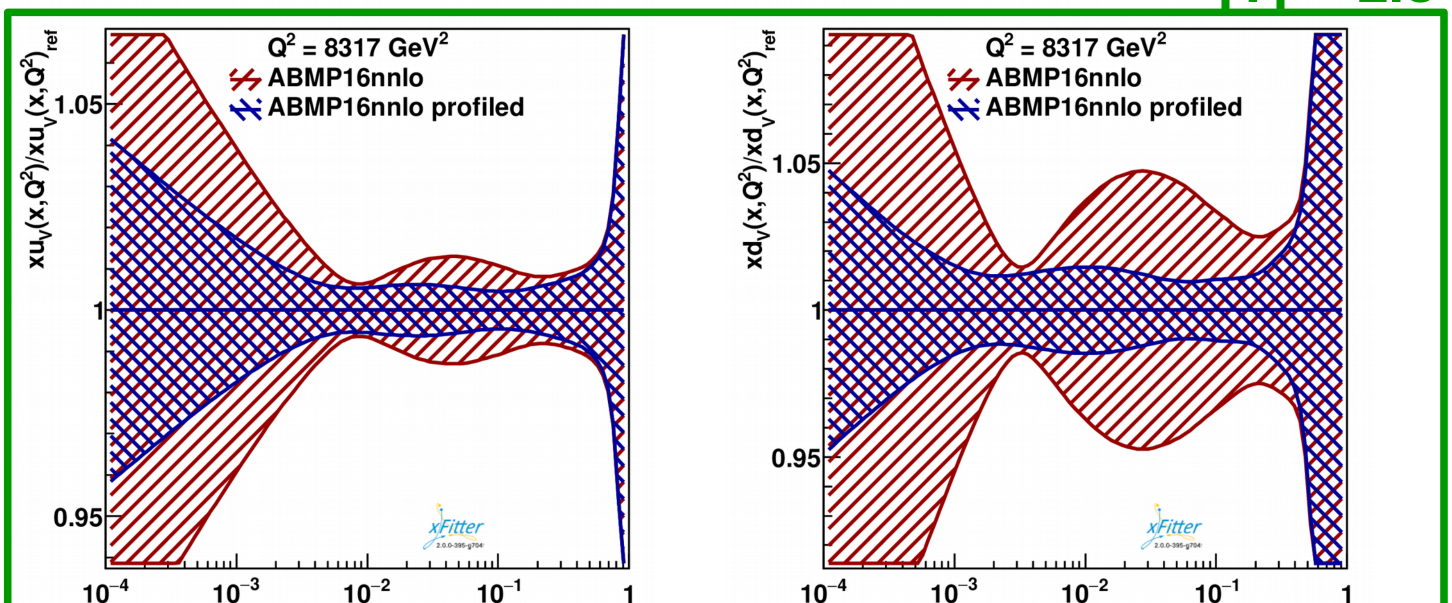

PDF eigenvectors rotation

ABMP16nnlo ($Q^2 = M_Z^2$ GeV^2) **(Symmetric Hessian eigenvectors)**

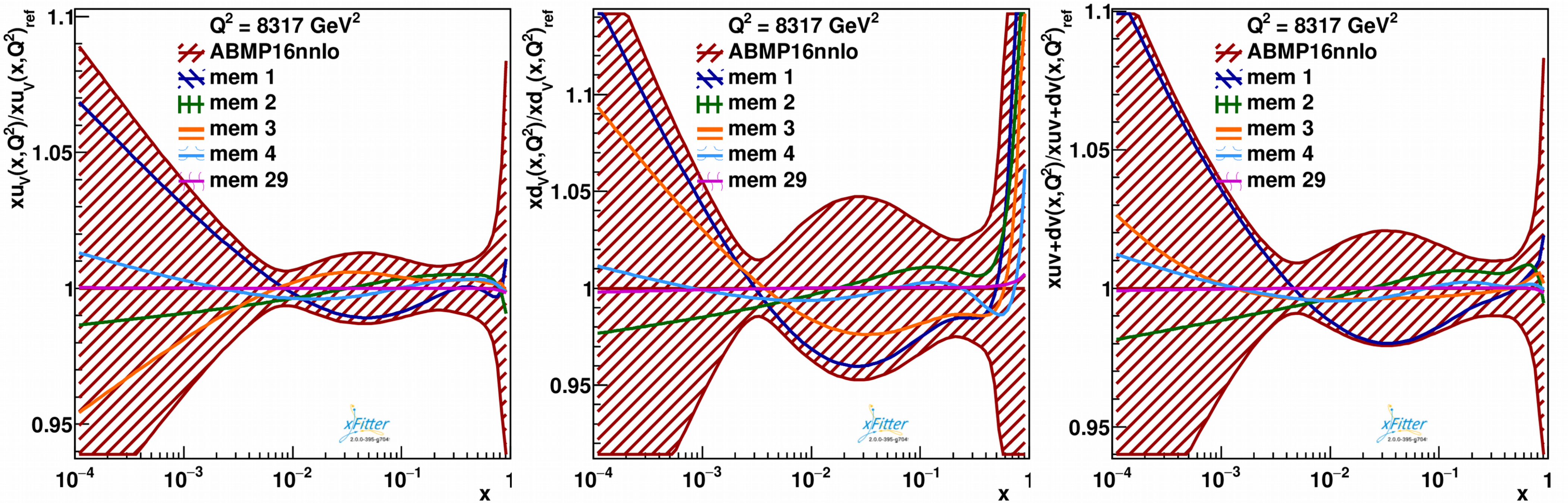

Dataset	ABMP16nnlo	mem 1	mem 2	mem 3	mem 4	mem 29
DY AFB	0 / 120	14 / 120	0.36 / 120	0.51 / 120	0.0100 / 120	0 / 120
Correlated χ^2	0.000000040	0	0	0	0	0
Log penalty χ^2	+0.00	-2.23	-0.09	-0.11	+0.00	+0.00
Total χ^2 / dof	0 / 120	12 / 106	0.27 / 106	0.40 / 106	0.0100 / 106	0 / 106
χ^2 p-value	1.00	1.00	1.00	1.00	1.00	1.00